NATIONAL ADVISORY COMMITTEE FOR AERONAUTICS

TECHNICAL NOTE

No. 1406

HIGH-SPEED WIND-TUNNEL TESTS OF AN NACA 16-009 AIRFOIL HAVING A 32.9-PERCENT-CHORD FLAP WITH AN OVERHANG 20.7 PERCENT OF THE FLAP CHORD

By David B. Stevenson and Robert W. Byrne

Langley Memorial Aeronautical Laboratory
Langley Field, Va.

Washington

August 1947

NATIONAL ADVISORY COMMITTEE FOR AERONAUTICS

TECHNICAL NOTE NO. 1406

HIGH-SPEED WIND-TUNNEL TESTS OF AN NACA 16-009 AIRFOIL HAVING A 32.9-PERCENT-CHORD FLAP WITH AN OVERHANG OF 20.7 PERCENT OF THE FLAP CHORD

By David B. Stevenson and Robert W. Byrne

SUMMARY

An investigation was conducted to determine the effects of compressibility upon the aerodynamic characteristics of a 5-inch-chord NACA 16-009 airfoil section having a 32.9-percent-chord flap with a 20.7-percent flap-chord nose overhang and a 1.8-percent-chord unsealed gap. Airfoil lift and pitching moment and flap hinge moments were obtained over an 8° angle-of-attack range and a flap angle range of 14° from a Mach number of 0.4 up to the maximum (choking) Mach numbers that could be attained for each model configuration.

The results showed that the elevator effectiveness decreased with increasing Mach number and that flap balance increased rapidly with increasing Mach number. Additional data obtained with the airfoil leading edge roughened indicated a serious loss in the rate of change of airfoil lift with flap angle for small flap deflections at all subcritical speeds and a large increase in the flap overbalance. Beyond the critical Mach number abrupt changes occurred in the aerodynamic effects produced by deflection of the flap.

INTRODUCTION

Reports on the performance of high-speed fighter airplanes and recent wind-tunnel investigations at high Mach numbers have indicated large adverse changes in control characteristics due to the effects of compressibility. The tests on a 5-inch-chord two-dimensional flapped NACA 16-009 airfoil reported herein are the first of a series of tests being conducted in the Langley 24-inch high-speed tunnel to investigate these effects.

SYMBOLS

M	stream Mach number
c_l	airfoil section lift coefficient
$c_{m_{c/4}}$	airfoil section pitching-moment coefficient about the quarter-chord point
c_h	flap section hinge-moment coefficient; based on c_f
δ_f	flap deflection; negative deflection is upward
α	angle of attack
c_f	flap chord behind the hinge line
c	chord of airfoil; zero flap deflection
ϕ	flap trailing-edge angle
R	radius

When α, δ_f, and c_l are used as subscripts outside the parentheses, they signify that the quantity is held constant.

APPARATUS AND TESTS

The tests were conducted in the Langley 24-inch high-speed tunnel, a closed-throat tunnel described in reference 1. Recent modification to this tunnel which reduced the model span exposed to the air stream from 24 to 18 inches is described in reference 2.

The model, which was made of steel, was a symmetrical airfoil with an NACA 16-009 profile modified to have a 32.9-percent-chord flap with an overhang of 20.7 percent of the flap chord. The 1.8-percent-chord gap was unsealed. A cross section of the model is shown as figure 1. The airfoil ordinates, except for the part affected by the flap nose shape, may be found in reference 3. The airfoil completely spanned the test section, passing through holes in the end plates in the tunnel walls. (See fig. 2.) These holes had the same shape as the airfoil profile, but were slightly larger than the model in order to provide clearance.

Airfoil lift and pitching moment were obtained by means of a spring-type balance similar to that described in reference 4. Flap hinge moments were measured by means of an electrical strain-gage system mounted on the balance.

The forces and moments were measured over an angle-of-attack range extending from -2° to 6° and a flap deflection range from -9.7° to 4.3°.

At an angle of attack of 0° and at flap deflections from -1.7° to -9.7° additional tests were made with carborundum particles (0.003 to 0.005 inch maximum dimension) embedded in a coat of shellac which had been applied to the upper and lower surfaces over a width extending from the leading edge to approximately the 8-percent-chord station. These tests were made to simulate an operating condition in which boundary-layer transition occurs near the leading edge. In full-scale installations this condition frequently exists either as a result of air-stream turbulence or surface irregularities or both.

The Mach number range for which the tests were made extended approximately from 0.40 to 0.85 corresponding to Reynolds numbers from approximately 1,100,000 to 1,900,000.

FACTORS AFFECTING TEST RESULTS

Tunnel-Wall Effects

Since tunnel-wall corrections are known from both theory and experiment to be small in the subcritical speed range for the small ratio of model to tunnel size of this investigation and since no rigorous correction has as yet been determined for the supercritical speed range, the force test data are presented uncorrected for the effects of the tunnel walls. As shown in reference 2, an important constriction effect in the supercritical speed range is an increase in the effective Mach number to a value greater than that used herein, which is the Mach number of the tunnel air stream just ahead of the model. Near the limiting, or choking, Mach number, however, even more serious constriction effects occur, as discussed in reference 2. In the present tests surveys (similar to those of reference 2) of the static pressure along the tunnel wall indicated the onset of these effects at Mach numbers approximately 0.02 to 0.03 below the choking Mach number. The data presented herein are, therefore, questionable within this speed range. In general, the highest Mach number for each model configuration shown in the figures corresponds to the choking condition.

Effect of End-Plate Gap

During the present tests leakage occurred between the test section and the surrounding test chamber through the end-plate gaps at the juncture between the model and the tunnel wall. The effect of this leakage upon lift and pitching-moment coefficient is shown in reference 1 by a comparison of force test data with end-plate gaps and essentially two-dimensional pressure-distribution data obtained in the Langley 24-inch high-speed tunnel. Although the absolute values obtained by the two methods differ to some extent, the results are in agreement as regards the effects of compressibility and therefore no correction for end leakage has been applied to the data presented herein.

Humidity Effects

At the higher tunnel speeds the relative humidity of the atmosphere, from which the air in the tunnel is drawn (reference 1), was found to affect the lift and moments under certain conditions. However, a value of relative humidity has been determined below which no measurable effects exist. The high-speed data contained herein were obtained with relative humidities less than this value.

RESULTS AND DISCUSSION

Lift

The effect of compressibility on the lift characteristics for constant angle of attack and flap angle is presented in figure 3. The radical changes in lift characteristics shown at supercritical Mach numbers undoubtedly include tunnel-wall effects, since the Mach numbers involved are near the choking condition. These effects, however, are believed to be illustrative of the type of phenomenon likely to occur at high supercritical speeds. Effects of this nature are caused by rapid pressure changes accompanying the rearward movement of the shock over the airfoil.

The section lift coefficient is shown as a function of angle of attack for various Mach numbers in figure 4. The variations with Mach number in these lift curves are considered normal for this airfoil section.

For small flap deflections ($\pm 2^\circ$) normal decrease in $(\partial c_l/\partial \delta_f)_\alpha$ occurred at very high speed. (See fig. 5(a).) An increasing loss in slope as the flap is deflected further at these speeds is evident.

With still greater deflection of the flap, however, the slopes become even greater than the low-speed values. These effects might be partly attributable to the peculiarities of the section at the low Reynolds numbers of these tests, but a decrease in slope for small flap angles followed by an increase in slope at higher flap angles has been found in other instances at supercritical Mach numbers.

The data of figure 5(b) show that the leading-edge roughness resulted in marked reduction in the $(\partial c_l/\partial \delta_f)_\alpha$ for small flap deflections in the subcritical speed range. The rapid drop in $(\partial c_l/\partial \delta_f)_\alpha$ that occurred for the smooth model above a Mach number of 0.7 near $\delta_f = -5^\circ$ (fig. 5(a)) did not occur for the roughened model in the same flap-angle range. Also, the force changes at high Mach number were less severe for the rough model than for the smooth model as a result of the thicker boundary layer. However, due to the difference in the values of the local skin friction coefficients in turbulent flow at high and low Reynolds numbers, the flap boundary-layer conditions were possibly worse than those which exist at flight Reynolds number.

The lift-curve slopes of figure 6, which are for small angle-of-attack and flap-angle ranges, resulted in a flap effectiveness $(\partial \alpha/\partial \delta_f)_{c_l=0}$ of only 0.46 at a Mach number of 0.40 (fig. 7). The data of reference 5 indicate that this low value is the result of the combination of a large trailing-edge angle and an unsealed flap nose gap. With increasing speed serious loss of flap effectiveness occurred (fig. 7); $(\partial \alpha/\partial \delta_f)_{c_l=0}$ falls to 0.22 at a Mach number of 0.80, about one-half of its low-speed values.

Included in figure 7 for comparison with the results of the subject tests is the value of $(\partial \alpha/\partial \delta_f)_{c_l=0}$ obtained by an empirical method based on data from tests at Mach numbers near 0.1 and at Reynolds numbers which were higher than those obtained in the present investigation. (See reference 6.)

Pitching Moment

Variations in the quarter-chord moment coefficient with Mach number for constant angular conditions are shown in figure 8. The curves of moment coefficient against lift coefficient at constant flap deflection (fig. 9) indicate large center-of-pressure shifts for small lift increments near $c_l = 0.3$ even at low speed. In order to show the center-of-pressure shifts, at least qualitatively,

the values of $\left(\frac{\partial c_{m_{c/4}}}{\partial c_l}\right)_{\delta_f}$ were plotted for three lift coefficients in figure 10.

The quarter-chord moment coefficient is shown as a function of flap deflection in figure 11(a). There is a large difference between the moment coefficients for $\delta_f = -6^\circ$ and -8° at a Mach number of 0.8. The difference is produced both by a change in lift coefficient (fig. 3(b)) and by a rearward shift in the center of pressure for this 2° flap-angle increment. This trend, together with the fact that relatively high values of $(\partial c_l/\partial \delta_f)_\alpha$ were attained at flap deflections beyond -6° (fig. 5(a)), indicates that marked improvement in the flow over the flap occurred as it was deflected to the higher angles.

A comparison of parts (a) and (b) of figure 11 shows that the effect of the roughened leading edge was to decrease the moment coefficients and to reduce the severity of the changes in $c_{m_{c/4}}$ which occurred at very high speeds for medium flap deflection.

Hinge Moment

The effects of compressibility on the flap section hinge-moment coefficient for constant angular conditions are presented in figure 12. Pressure-distribution data and schlieren flow photographs obtained in the Langley rectangular high-speed tunnel in investigations of other flapped airfoils have shown that abrupt changes in hinge-moment coefficient occurred when the critical speed was exceeded. These effects were found to arise from the passage of shock waves across the flap. The variations of hinge-moment coefficient with angle of attack for a flap angle of 0.3° and with flap deflection for an angle of attack of 0° are shown in figures 13 and 14, respectively. Comparison of figures 14(a) and 14(b) shows that the addition of roughness to the airfoil leading edge resulted in a large increase in the balance for all speeds. In this case, as was true for the lift and pitching moment, a less abrupt change in slope in passing from the low to high flap deflections (-4° to -8°) was obtained.

The variations with Mach number of $(\partial c_h/\partial \alpha)_{\delta_f}$ and $(\partial c_h/\partial \delta_f)_\alpha$ are given in figure 15. These slopes, each of which is the value for $\alpha = 0^\circ$ and $\delta = 0.3^\circ$, apply over a very limited range of angle of attack and flap deflection as is evident from figures 13 and 14. Estimated values of $(\partial c_h/\partial \alpha)_{\delta_f}$ and $(\partial c_h/\partial \delta_f)_\alpha$ obtained from empirical methods presented in reference 6 are included in figure 15.

Reference 6 shows that a small part of the total aerodynamic balance was due to the small nose overhang; the greater part was due to the high trailing-edge angle in the presence of an unsealed gap. The tendency for the flap balance to increase with increasing Mach number at subcritical speeds is believed to be a characteristic of flaps with relatively large trailing-edge angles, although a large flap nose gap probably augments this tendency. Much less increase and even a decrease in balance with Mach number has been found for models having various amounts of nose overhang with smaller trailing-edge angles. References 7 and 8, which present results of tests of three-dimensional models, show that for elevators having overhangs of 30 and 48 percent of the chord behind the hinge center line and trailing-edge angles of 12° and 13°, respectively, a decrease in balance with Mach number was found.

CONCLUSIONS

The results of the present high-speed wind-tunnel investigation of a 5-inch-chord NACA 16-009 airfoil having a 32.9-percent-chord flap with a 20.7-percent flap-chord nose overhang, and a 1.8-percent-chord unsealed gap can be summarized as follows:

1. The elevator-effectiveness factor $(\partial\alpha/\partial\delta_f)_{c_l=0}$ for small angle-of-attack and flap-angle increments for the smooth model was 0.46 at a Mach number of 0.4 but had decreased to a value of 0.22 at a Mach number of 0.8.

2. The aerodynamic balance for the flap tested increased with increasing Mach numbers in the subcritical speed range. Beyond the critical Mach number abrupt changes in the hinge-moment characteristics occurred.

3. The presence of roughness on the leading edge produced (a) a marked decrease in the rate of change of lift and quarter-chord moment coefficient with flap angle for small flap deflections, and (b) a large increase in the aerodynamic balance of the flap.

Langley Memorial Aeronautical Laboratory
National Advisory Committee for Aeronautics
Langley Field, Va., June 9, 1947

REFERENCES

1. Stack, John, Lindsey, W. F., and Littell, Robert E.: The Compressibility Burble and the Effect of Compressibility on Pressures and Forces Acting on an Airfoil. NACA Rep. No. 646, 1938.

2. Byrne, Robert W.: Experimental Constriction Effects in High-Speed Wind Tunnels. NACA ACR No. L4L07a, 1944.

3. Stack, John: Tests of Airfoils Designed to Delay the Compressibility Burble. NACA TN No. 976, Dec. 1944. (Reprint of ACR, June 1939.)

4. Stack, John: The N.A.C.A. High-Speed Wind Tunnel and Tests of Six Propeller Sections. NACA Rep. No. 463, 1933.

5. Purser, Paul E., and Riebe, John M.: Wind-Tunnel Investigation of Control-Surface Characteristics. XV -- Various Contour Modifications of a 0.30-Airfoil-Chord Plain Flap on an NACA 66(215)-014 Airfoil. NACA ACR No. 3L20, 1943.

6. Langley Research Department: Summary of Lateral-Control Research. (Compiled by Thomas A. Toll.) NACA TN No. 1245, 1947.

7. Schueller, Carl F., and Korycinski, Peter F.: Effect of Fabric Deflection at High Speeds on the Aerodynamic Characteristics of the Horizontal Tail Surface of an SB2D-1 Airplane. NACA ARR No. L5F01a, 1945.

8. Schueller, Carl F., Korycinski, Peter F., and Strass, H. Kurt: Tests of a Full-Scale Horizontal Tail Surface in the Langley 16-Foot High-Speed Tunnel. NACA TN No. 1074, 1946.

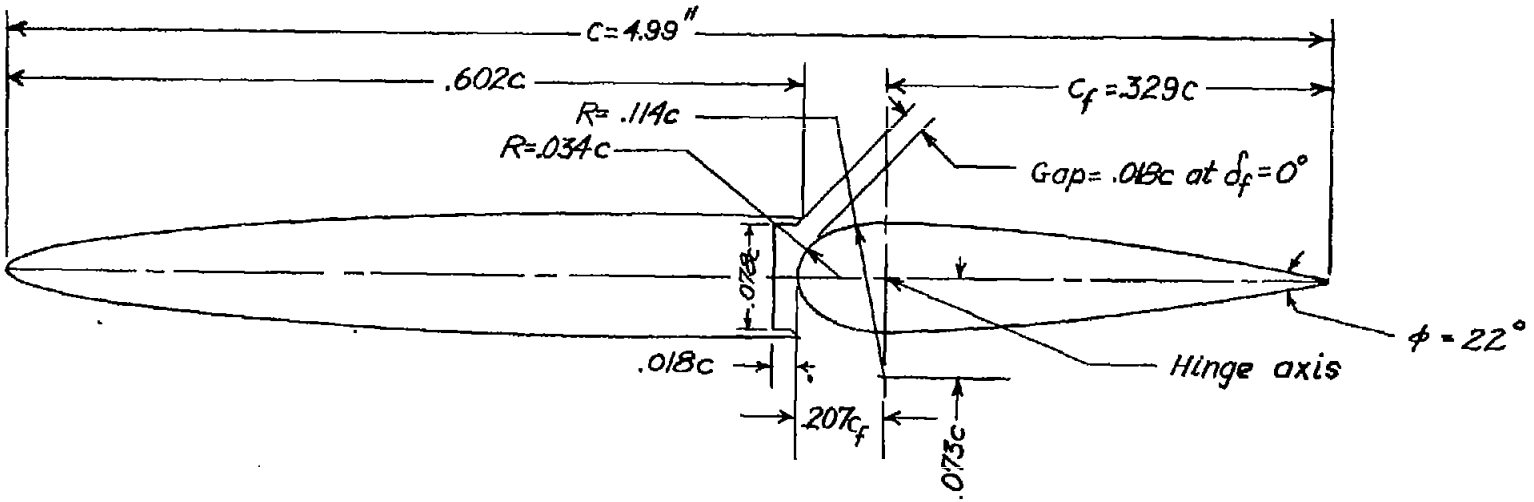

NATIONAL ADVISORY
COMMITTEE FOR AERONAUTICS

Figure 1.- NACA 16-009 airfoil with a 0.329c flap having a $0.207c_f$ nose overhang.

Figure 2.- Langley 24-inch high-speed-tunnel test section with access door removed.

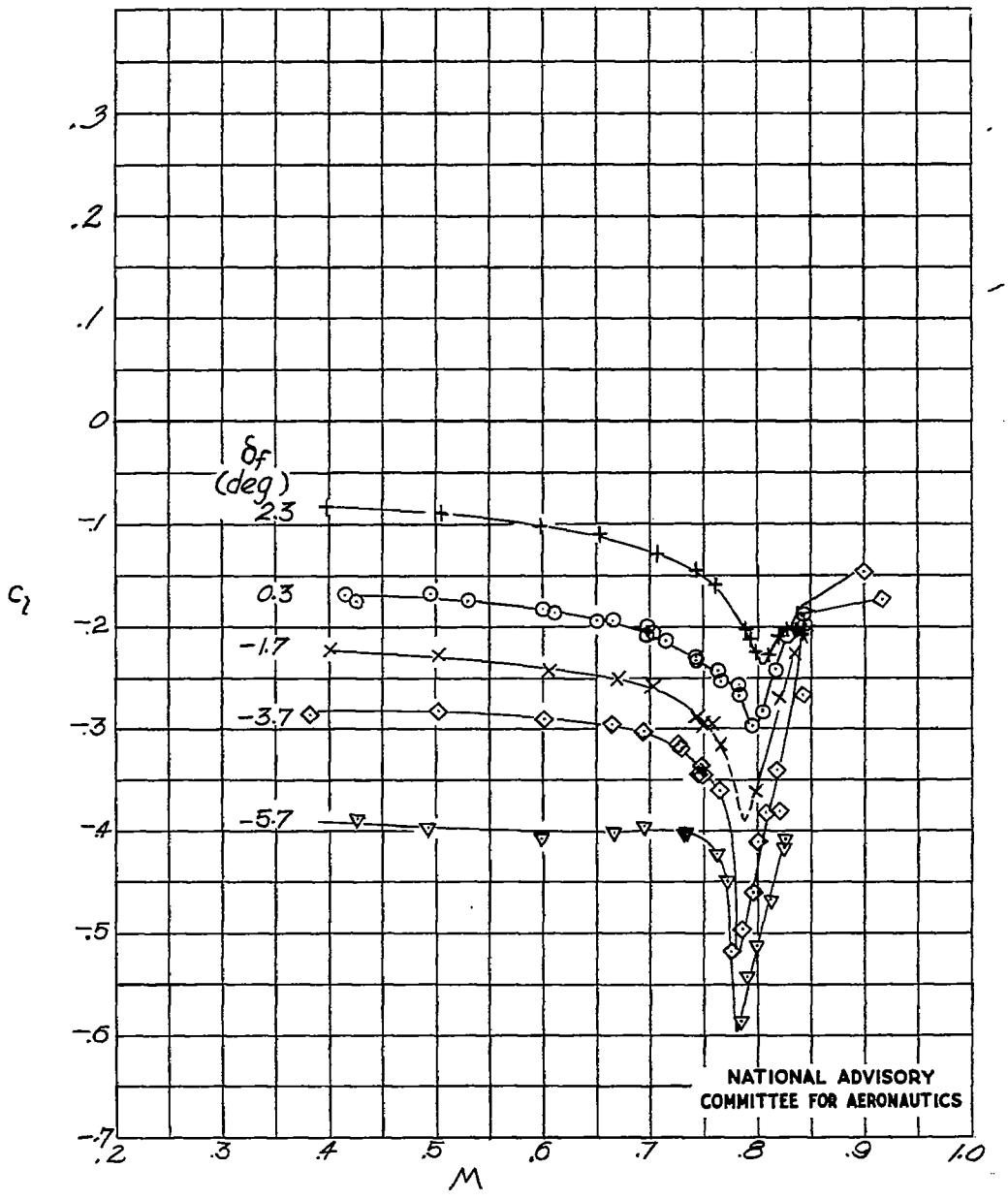

(a) $\alpha = -2^\circ$.

Figure 3.- Variation of section lift coefficient with Mach number.

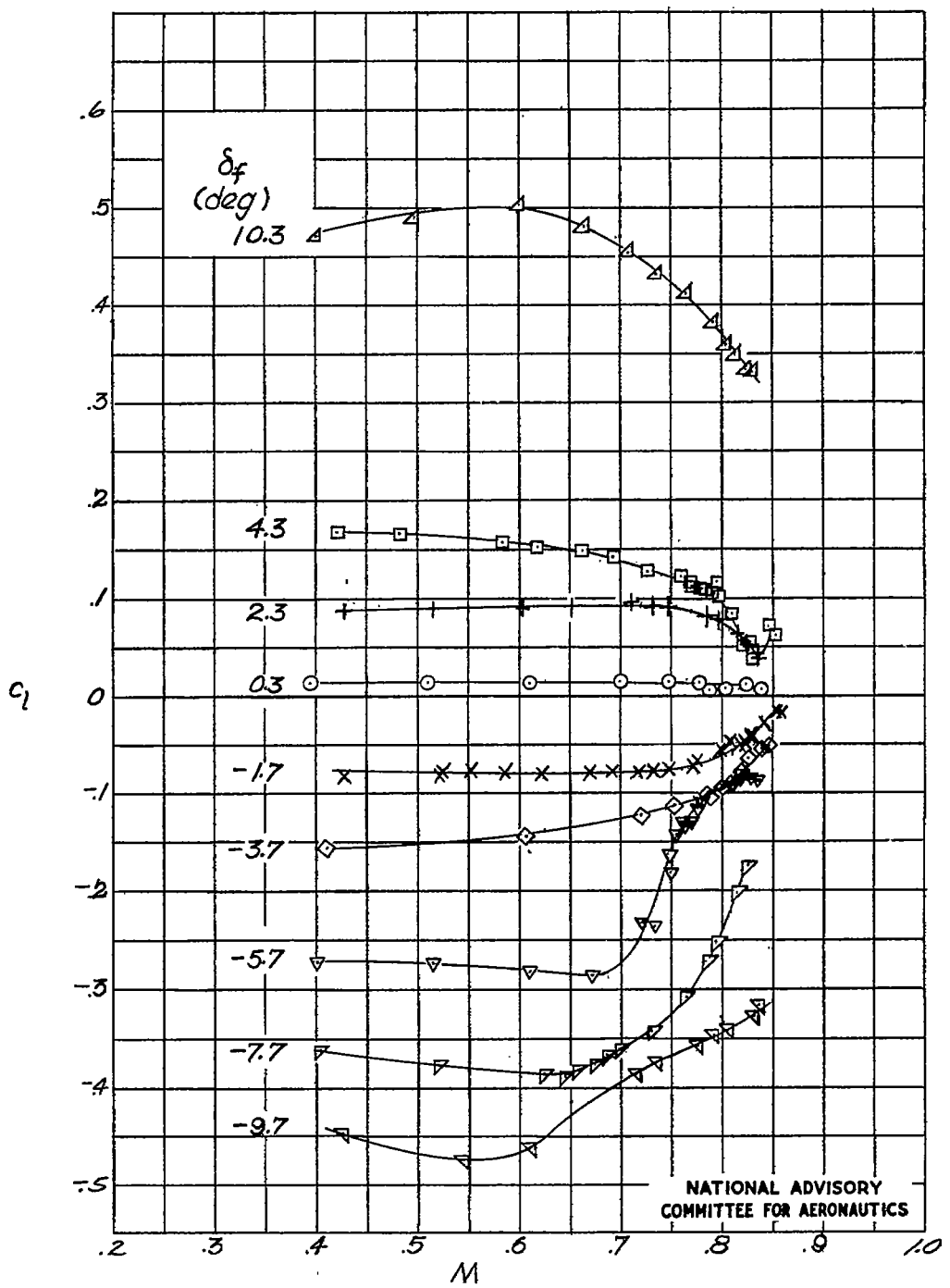

(b) $\alpha = 0^\circ$.

Figure 3.- Continued.

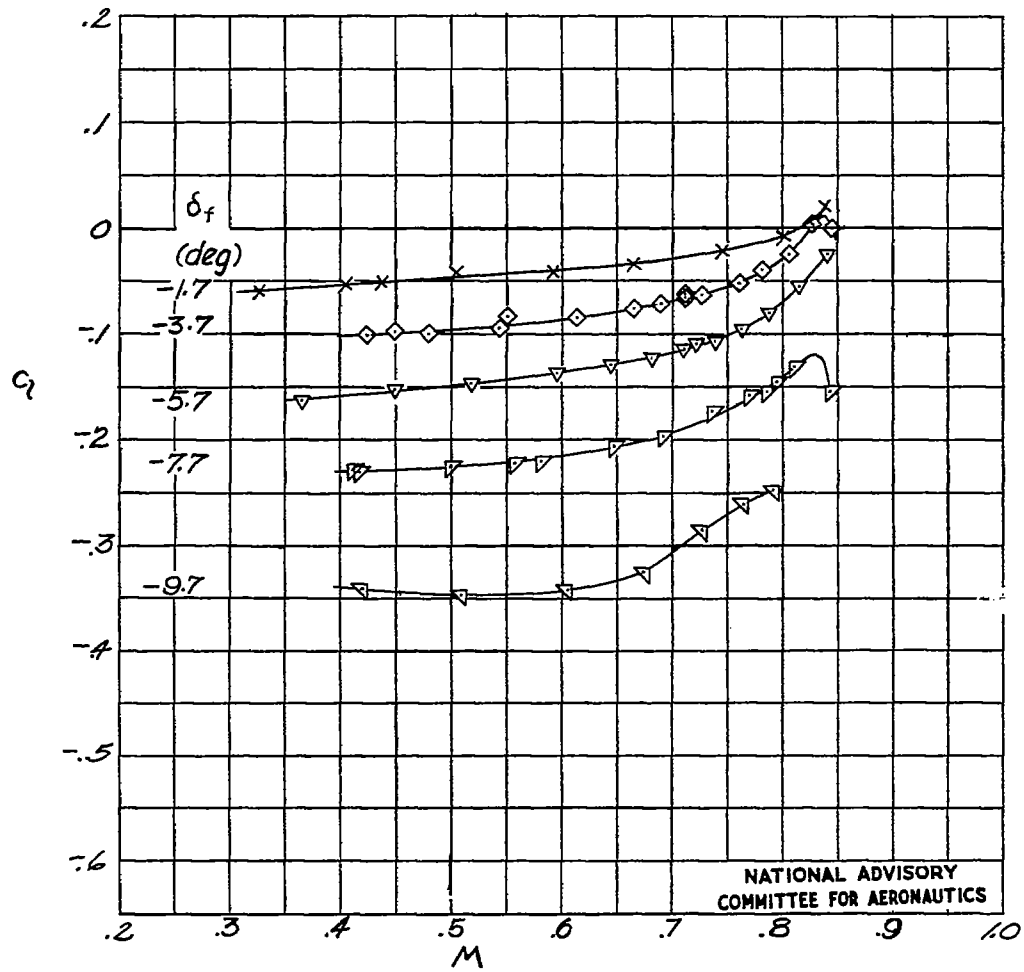

(c) $\alpha = 0^{\circ}$. Leading edge roughened.

Figure 3.- Continued.

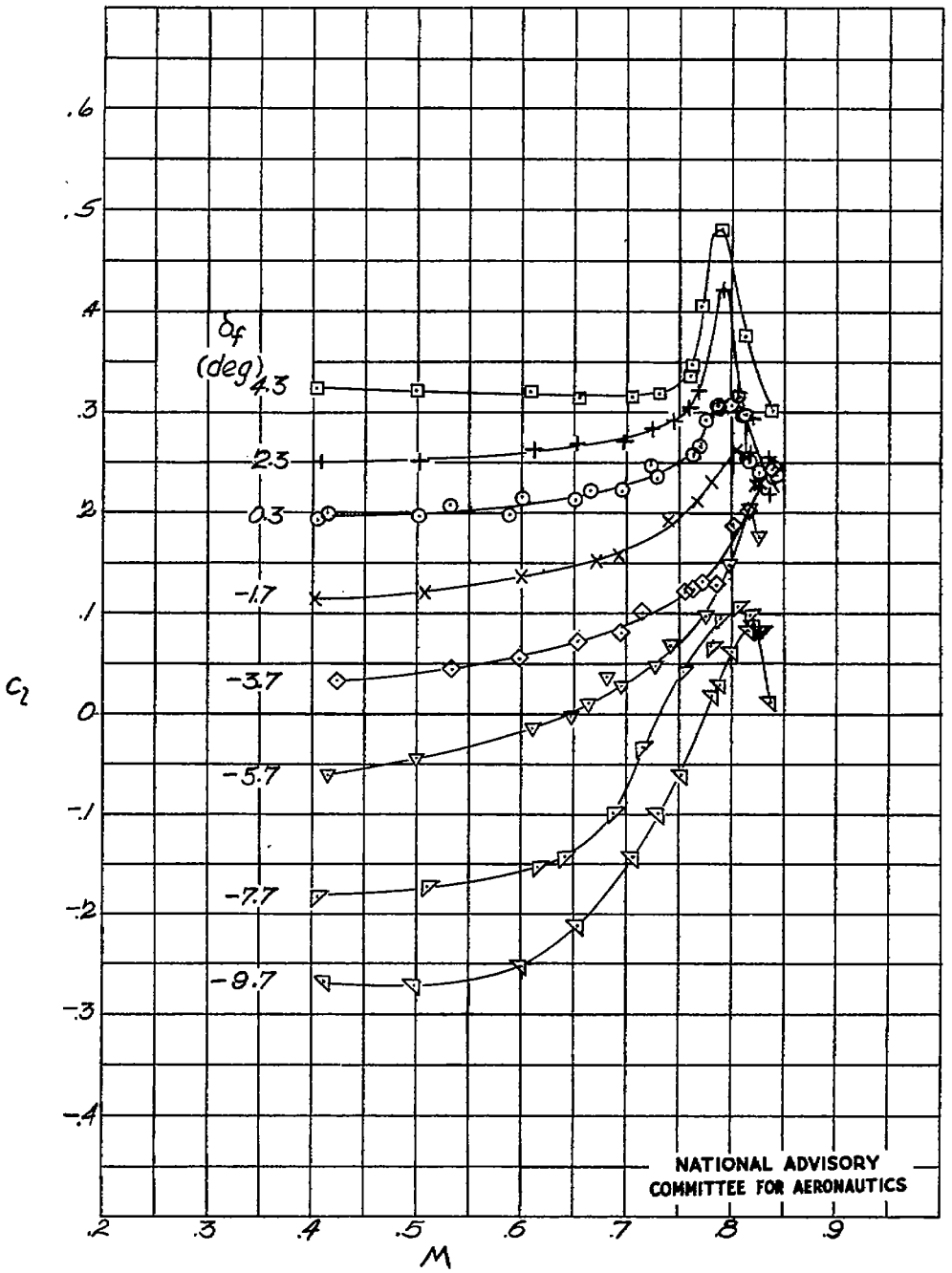

(d) $\alpha = 2^\circ$.

Figure 3.- Continued.

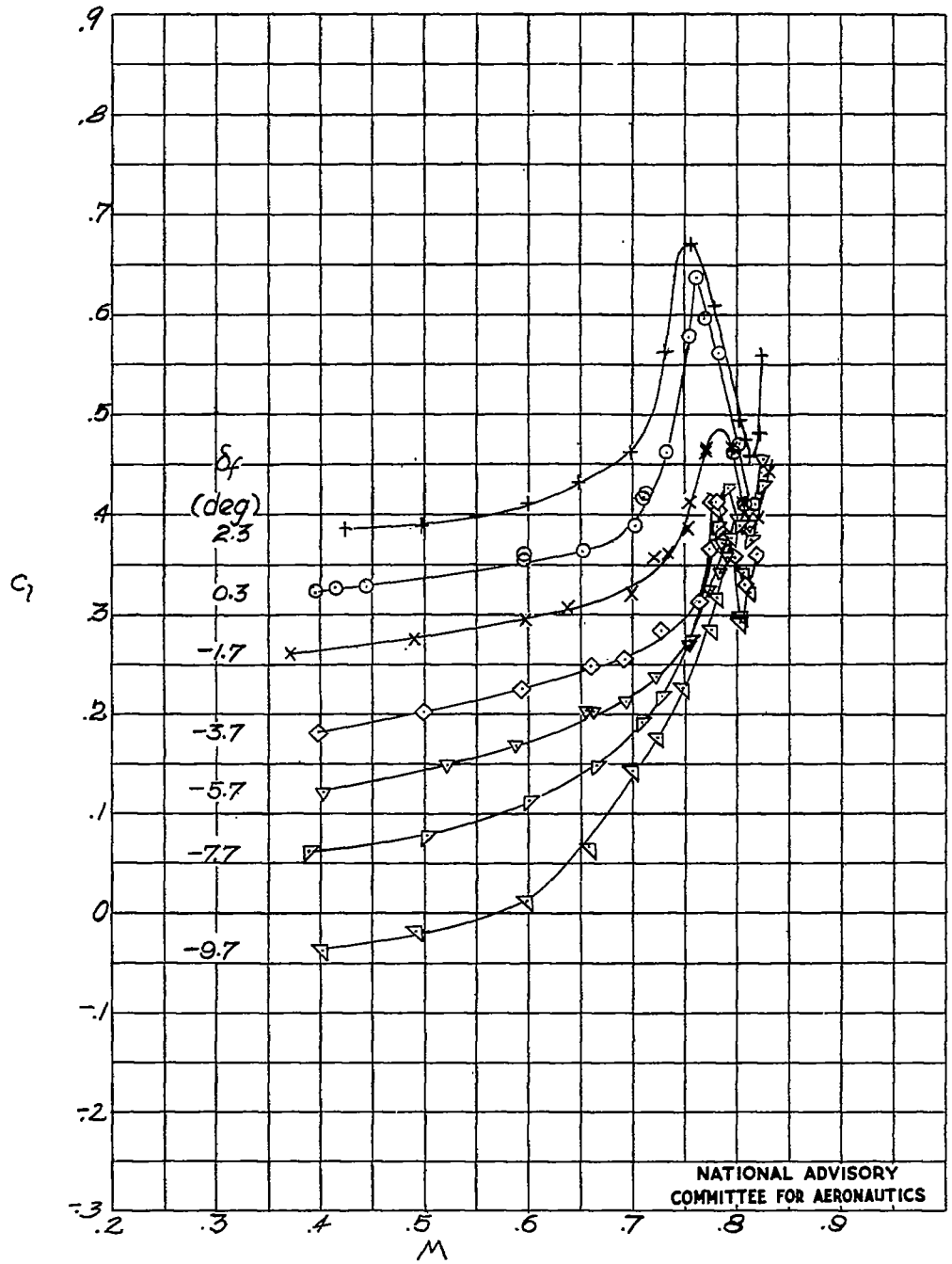

(e) $\alpha = 4^{\circ}$.

Figure 3.- Continued.

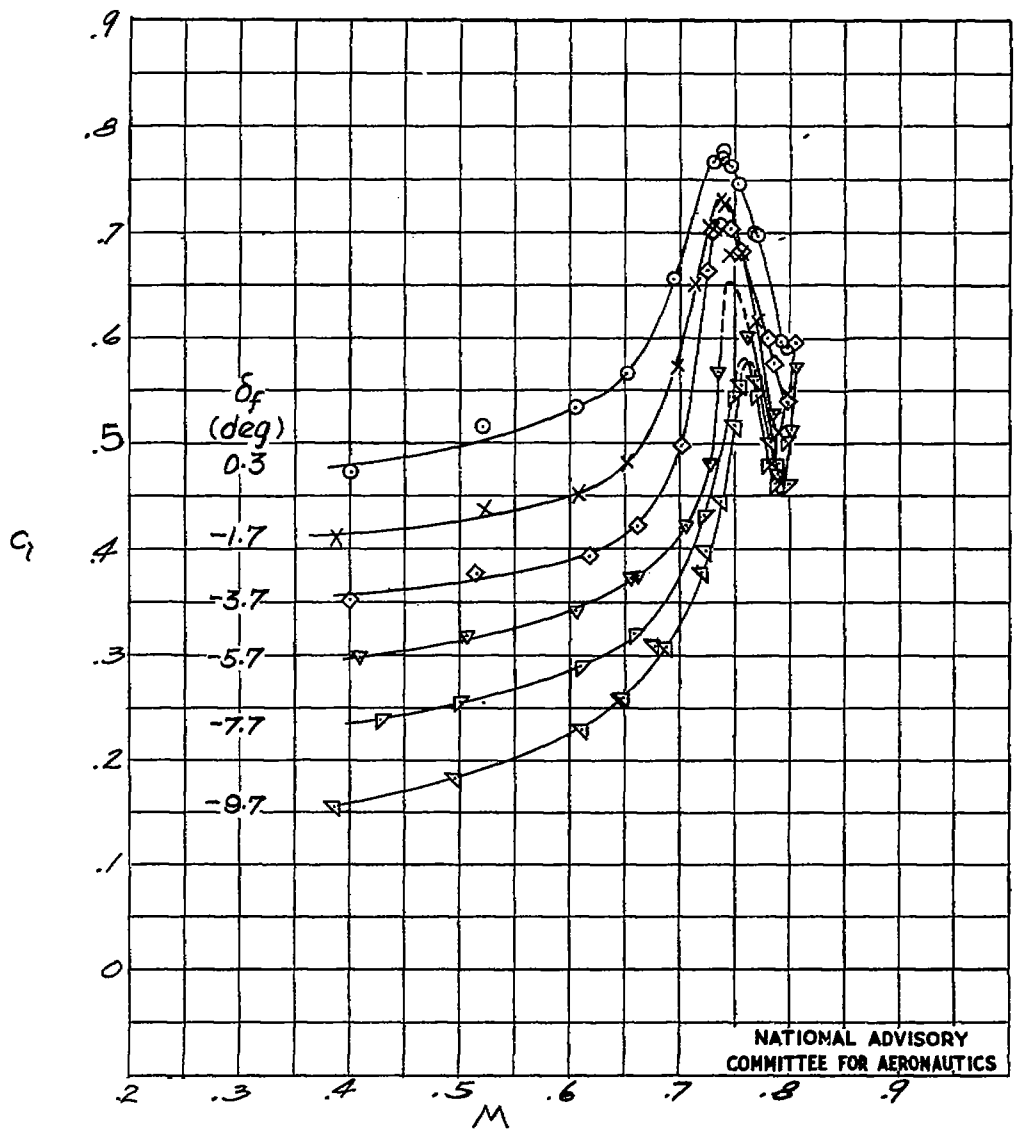

(f) $\alpha = 6^\circ$.

Figure 3.- Concluded.

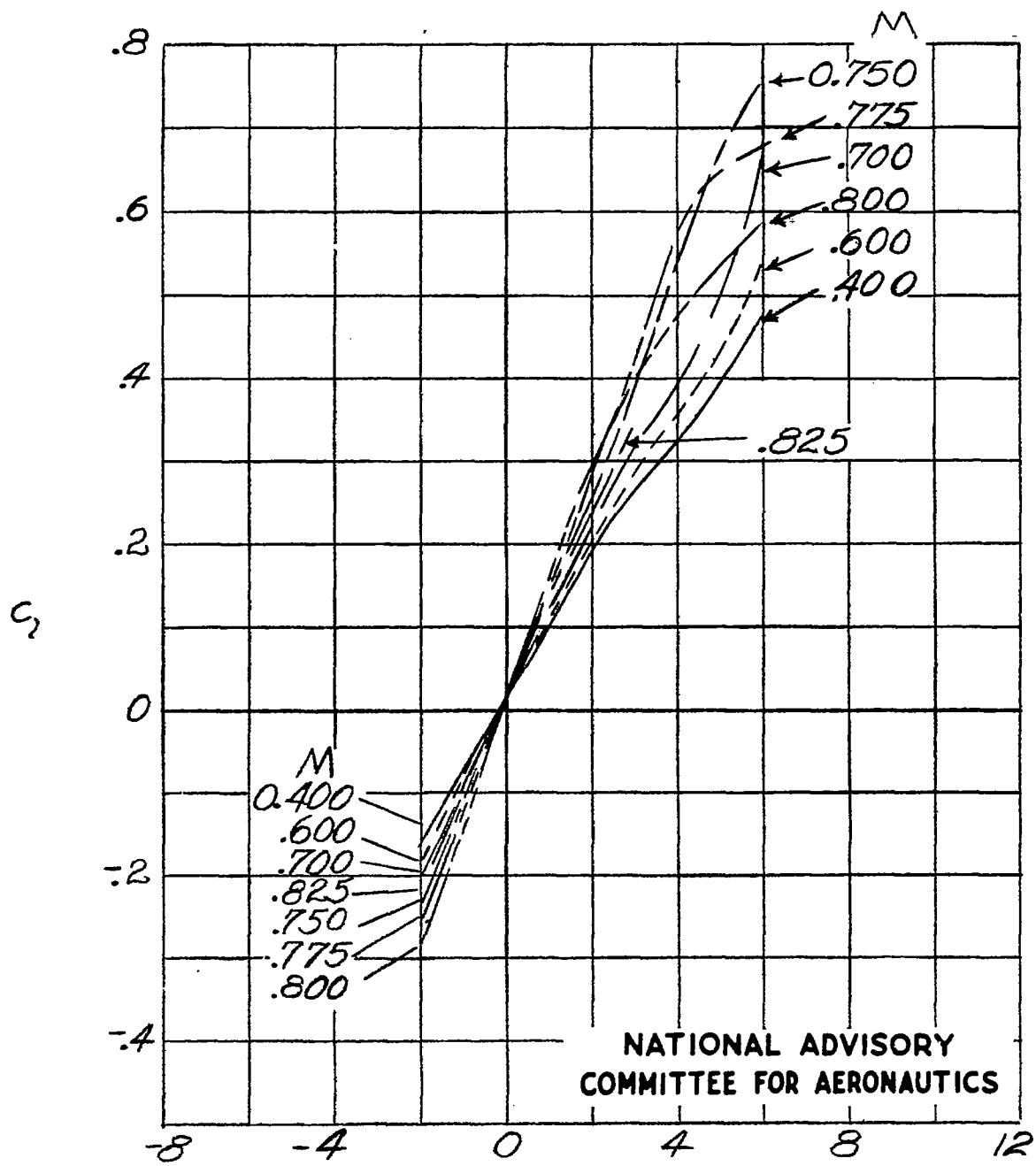

Angle of attack, α, deg

Figure 4.- Variation of section lift coefficient with angle of attack. $\delta_f = 0.3°$.

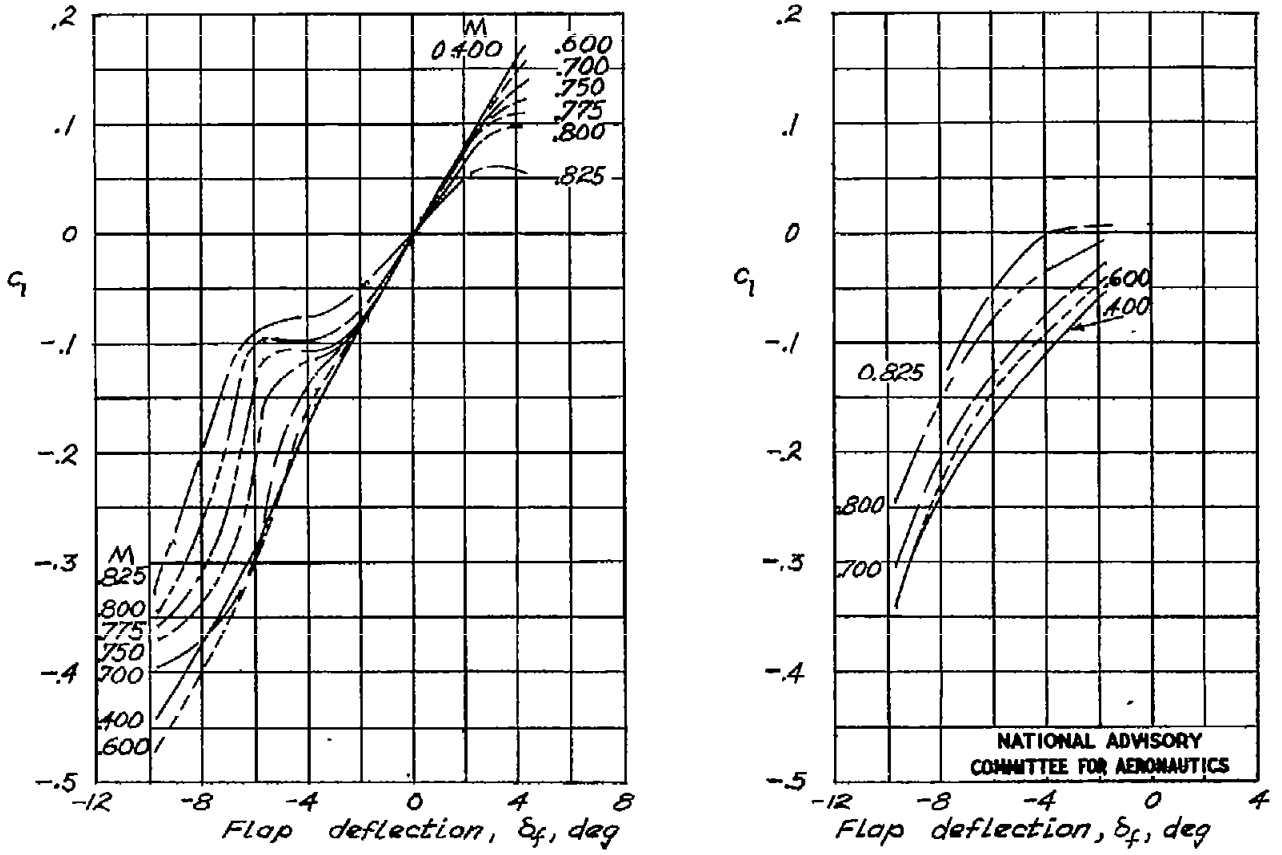

(a) $\alpha = 0^\circ$. (b) $\alpha = 0^\circ$. Leading edge roughened.

Figure 5.- Variation of section lift coefficient with flap deflection.

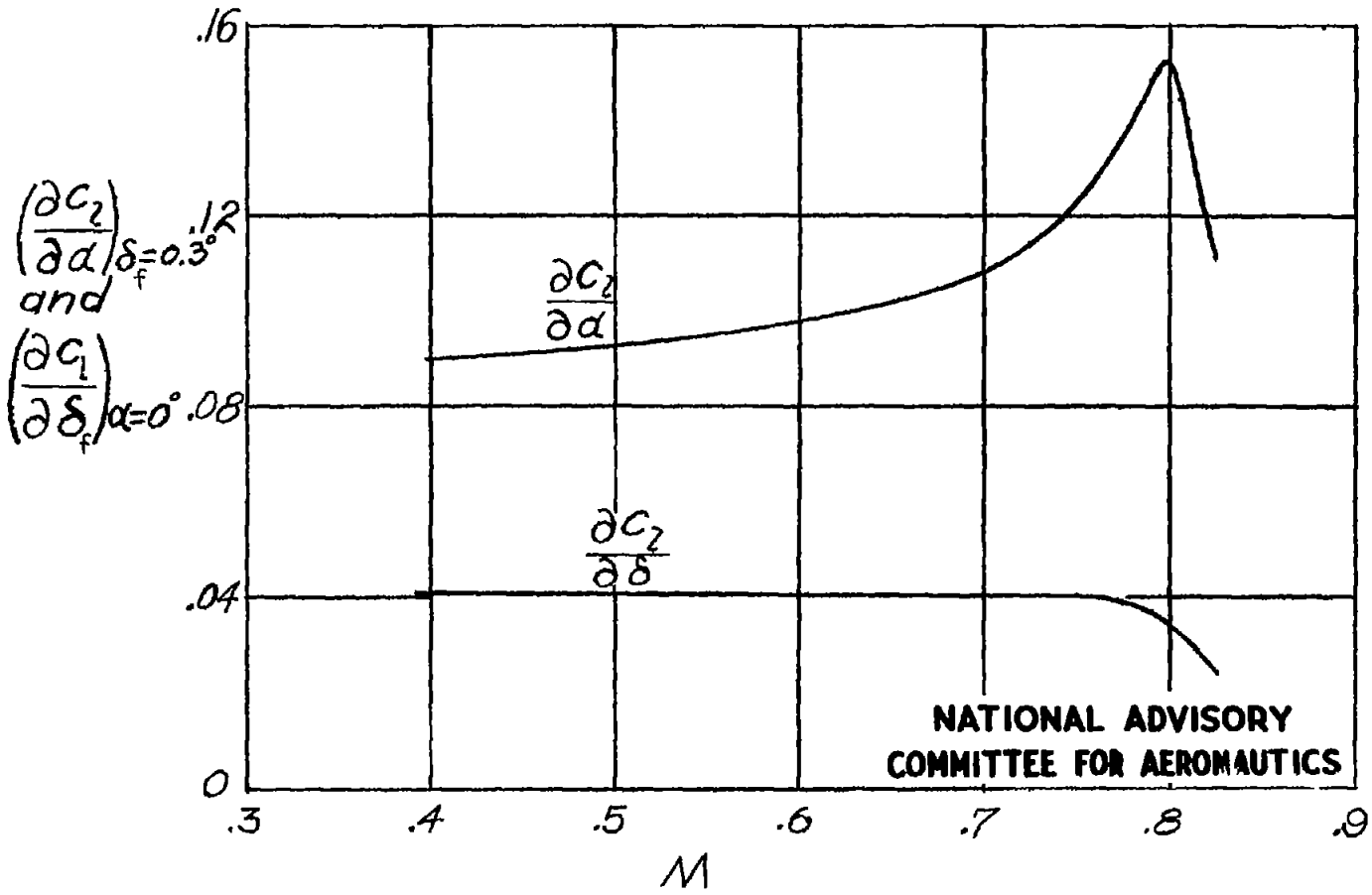

Figure 6.- Variation of lift-curve slopes with Mach number.

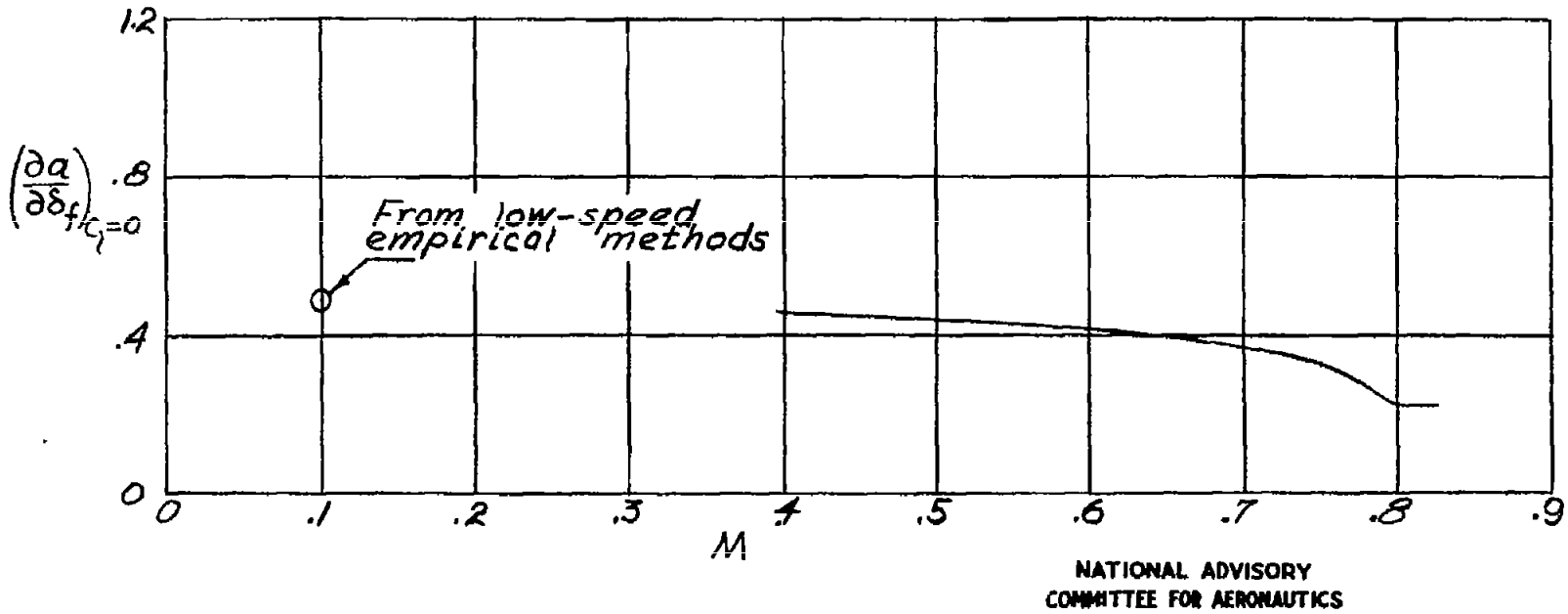

Figure 7.- Variation of flap effectiveness with Mach number.

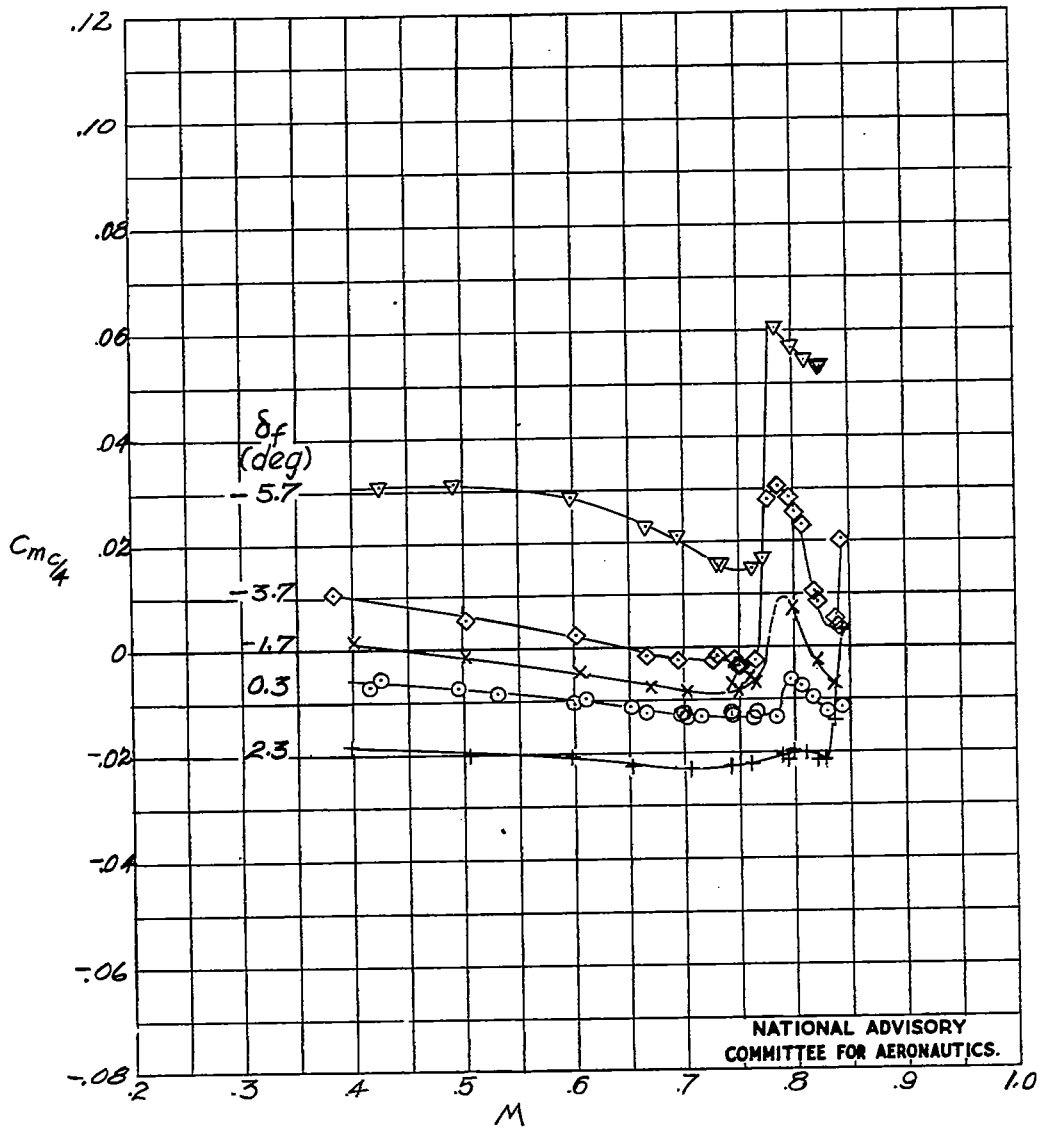

(a) $\alpha = -2^\circ$.

Figure 8.- Variation of section quarter-chord moment coefficient with Mach number.

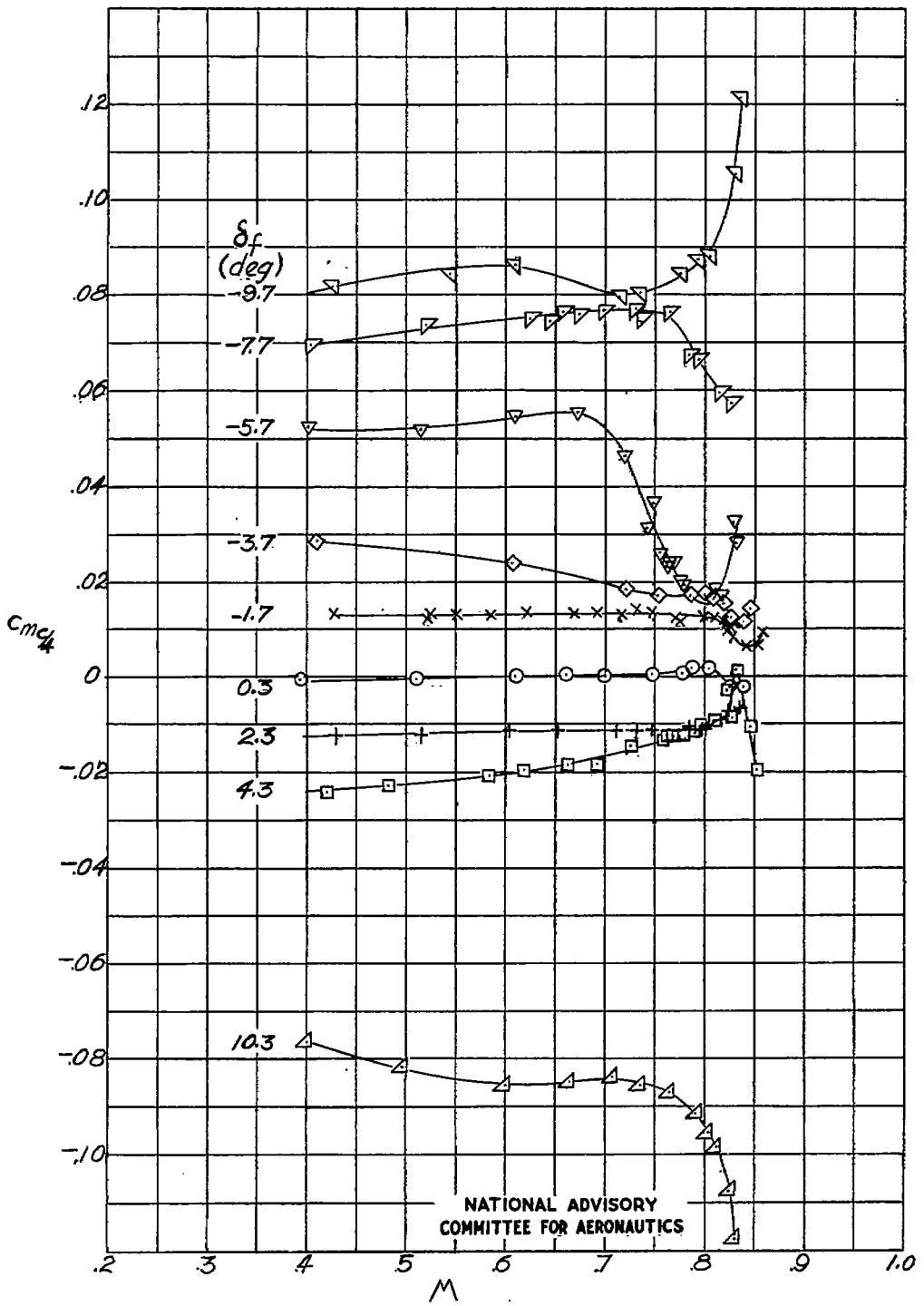

(b) $\alpha = 0°$.

Figure 8.- Continued.

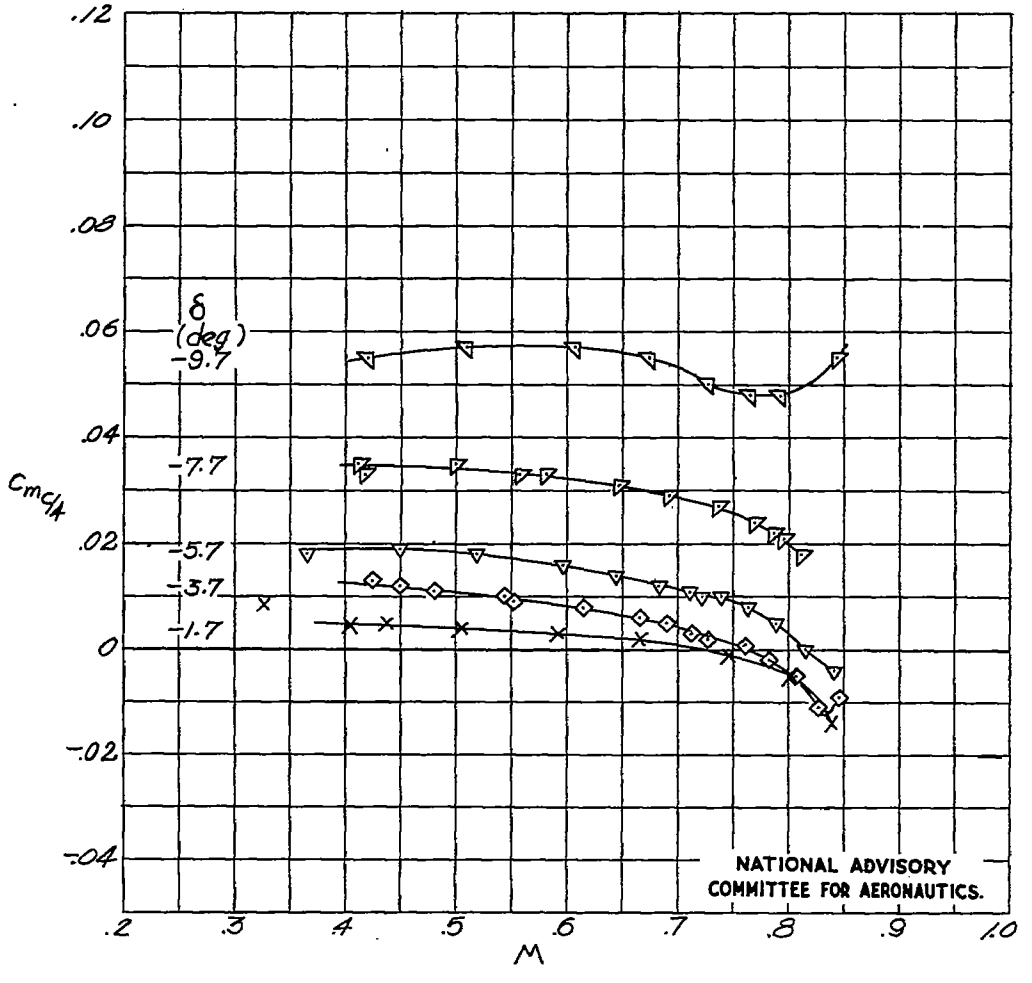

(c) $\alpha = 0^{\circ}$. Leading edge roughened.

Figure 8.- Continued.

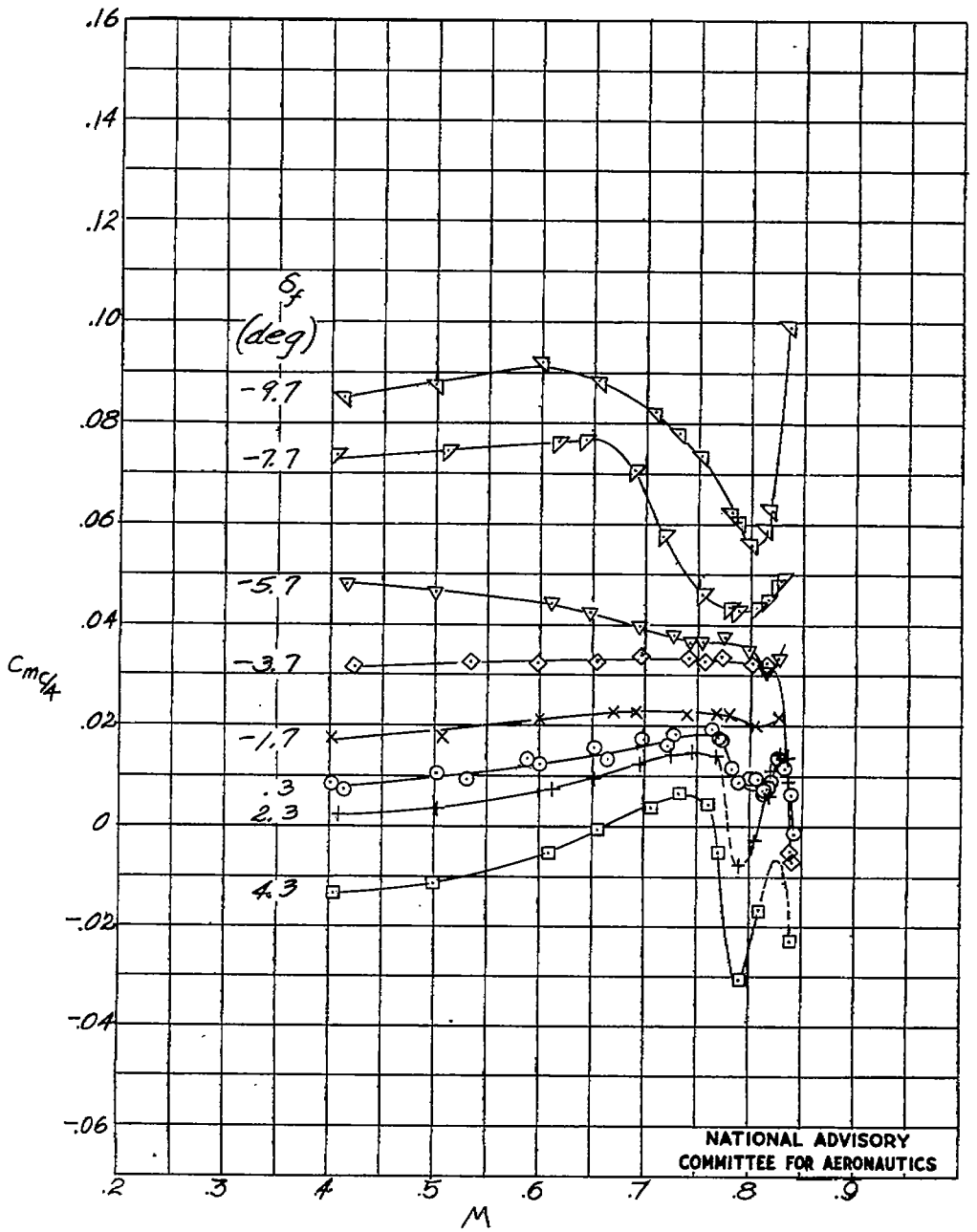

(d) $\alpha = 2^\circ$.

Figure 8.- Continued.

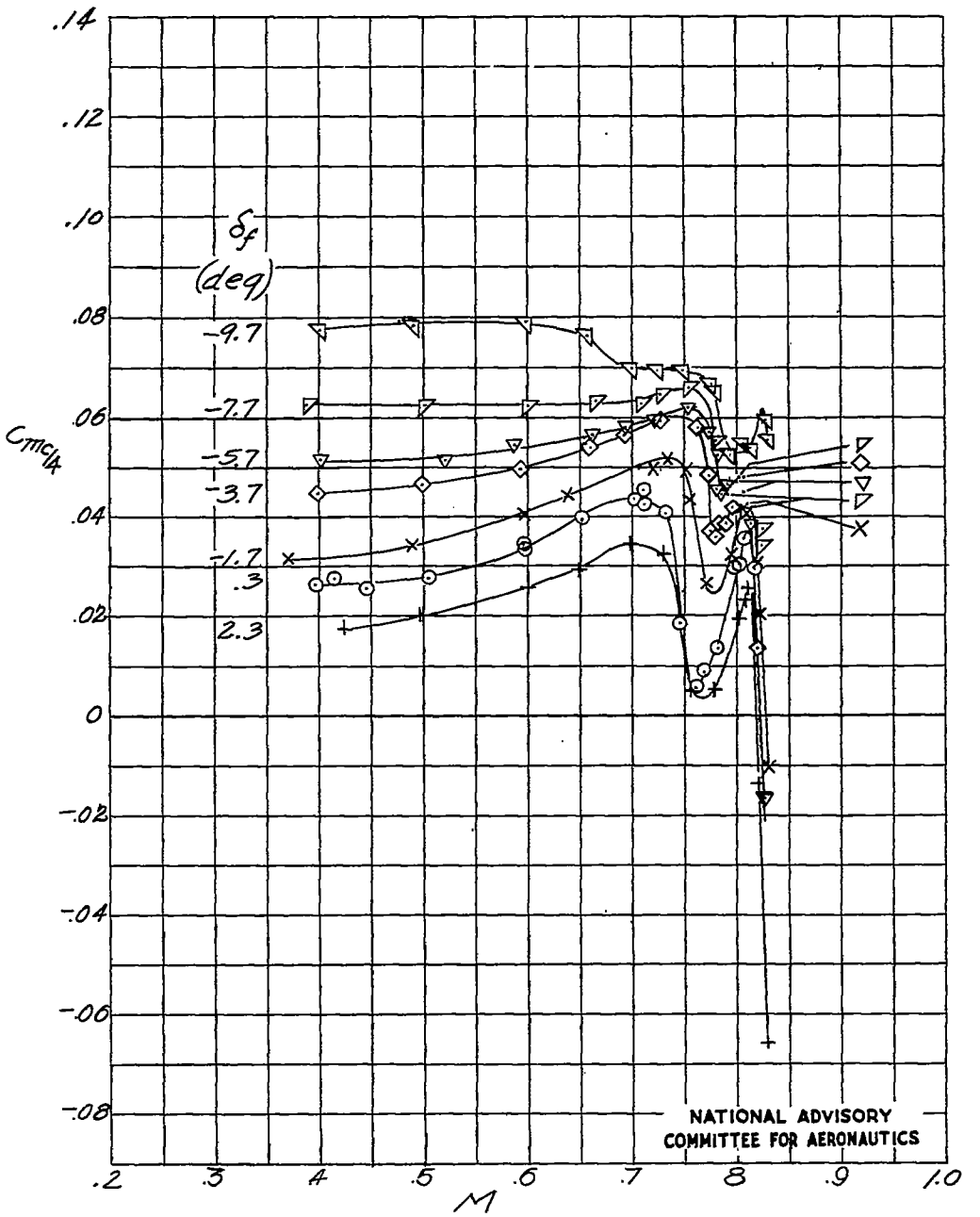

(e) $\alpha = 4^\circ$.

Figure 8.- Continued.

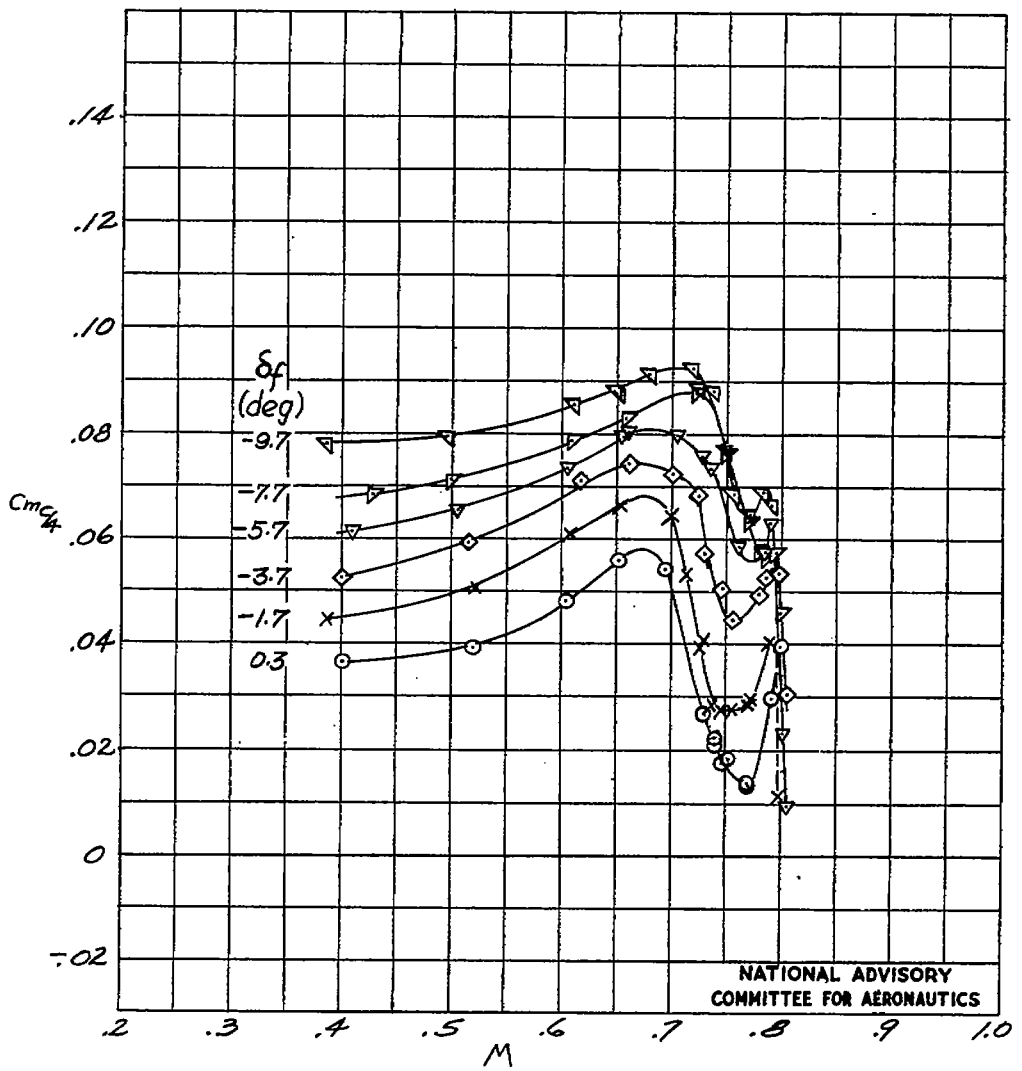

(f) $\alpha = 6^\circ$.

Figure 8.- Concluded.

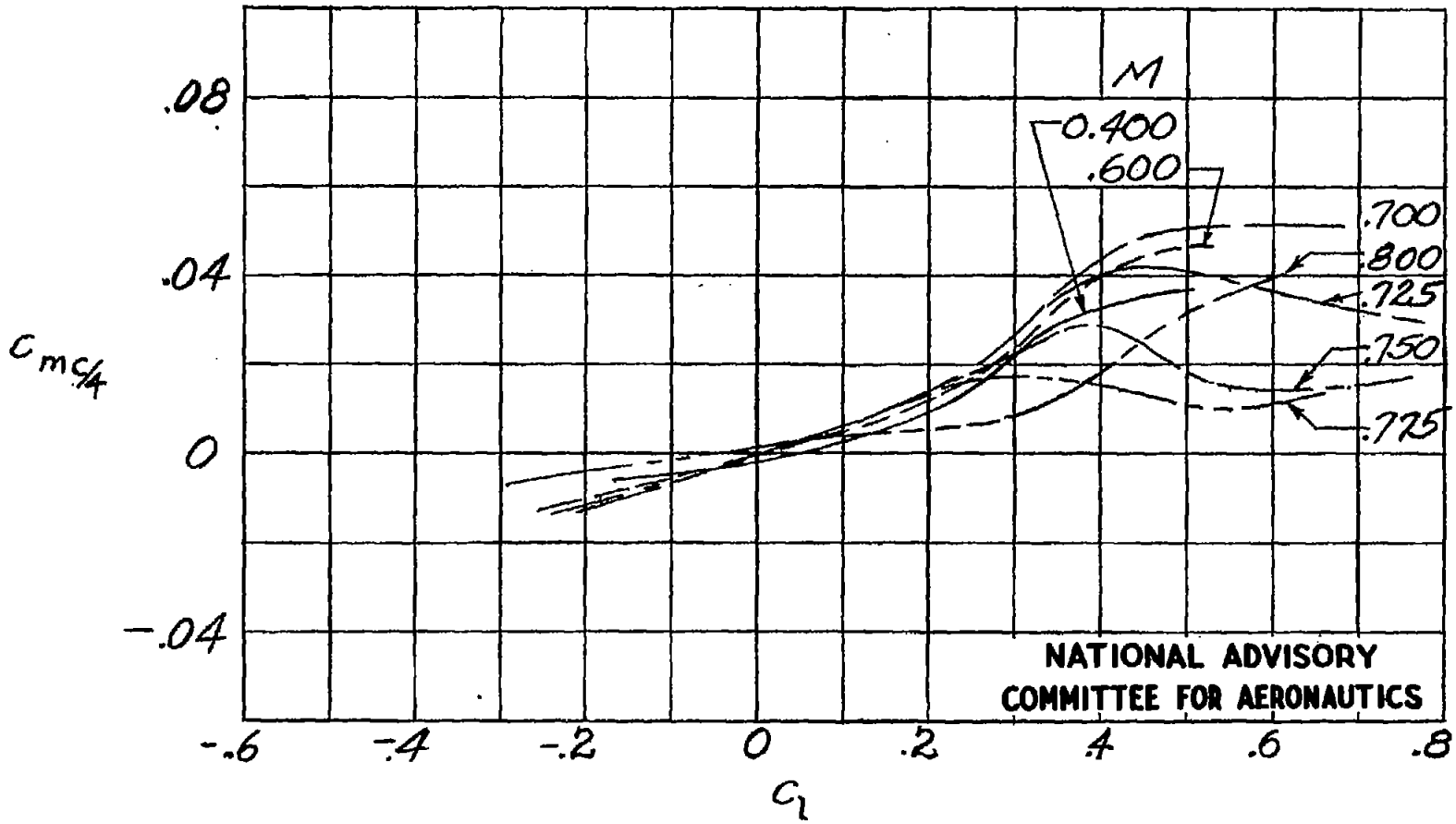

Figure 9.- Variation of section quarter-chord moment coefficient with section lift coefficient. $\delta_f = 0.3°$.

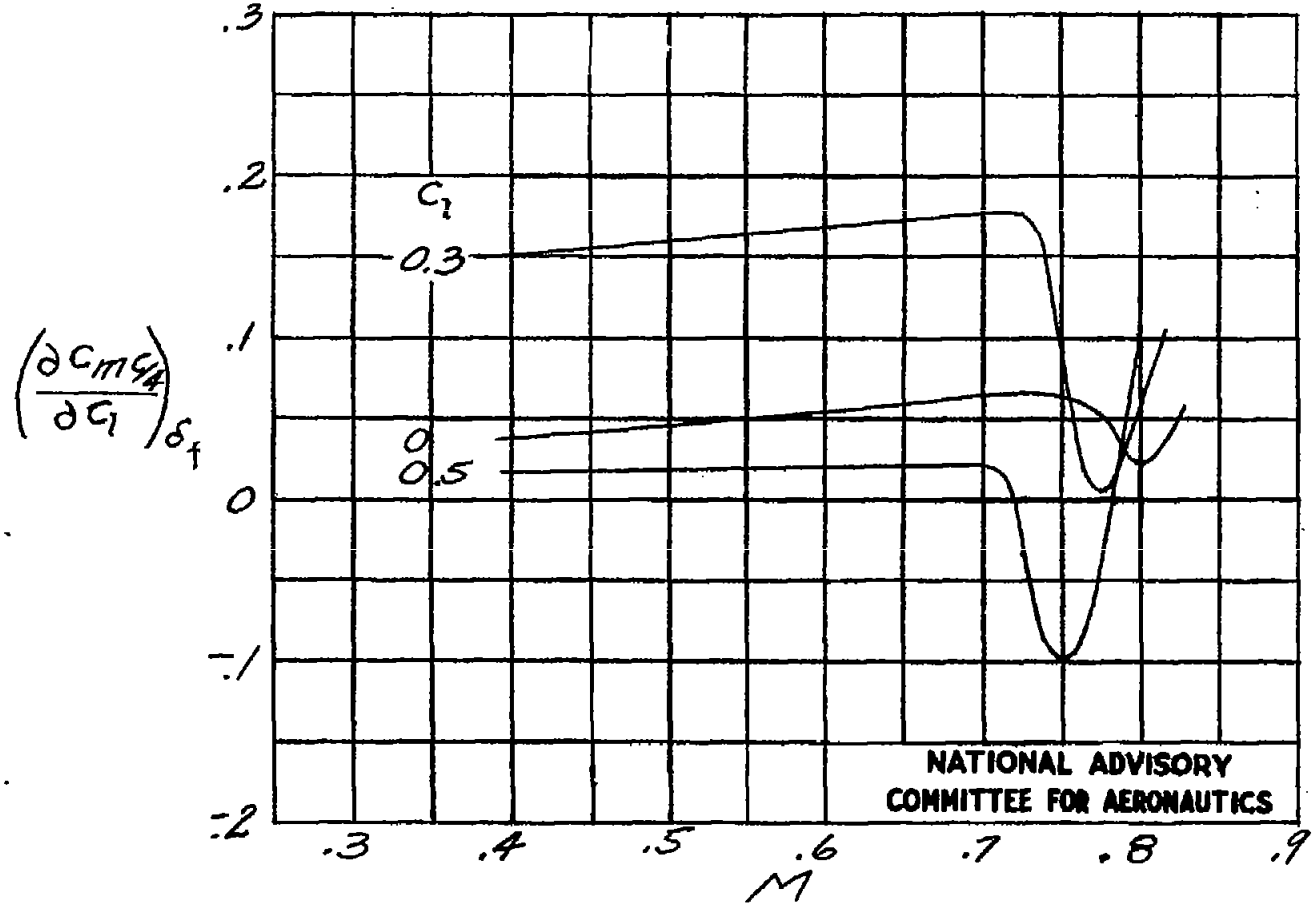

Figure 10.- Variation with Mach number of the rate of change of airfoil-section moment coefficient with section lift coefficient. $\delta_f = 0.3^\circ$.

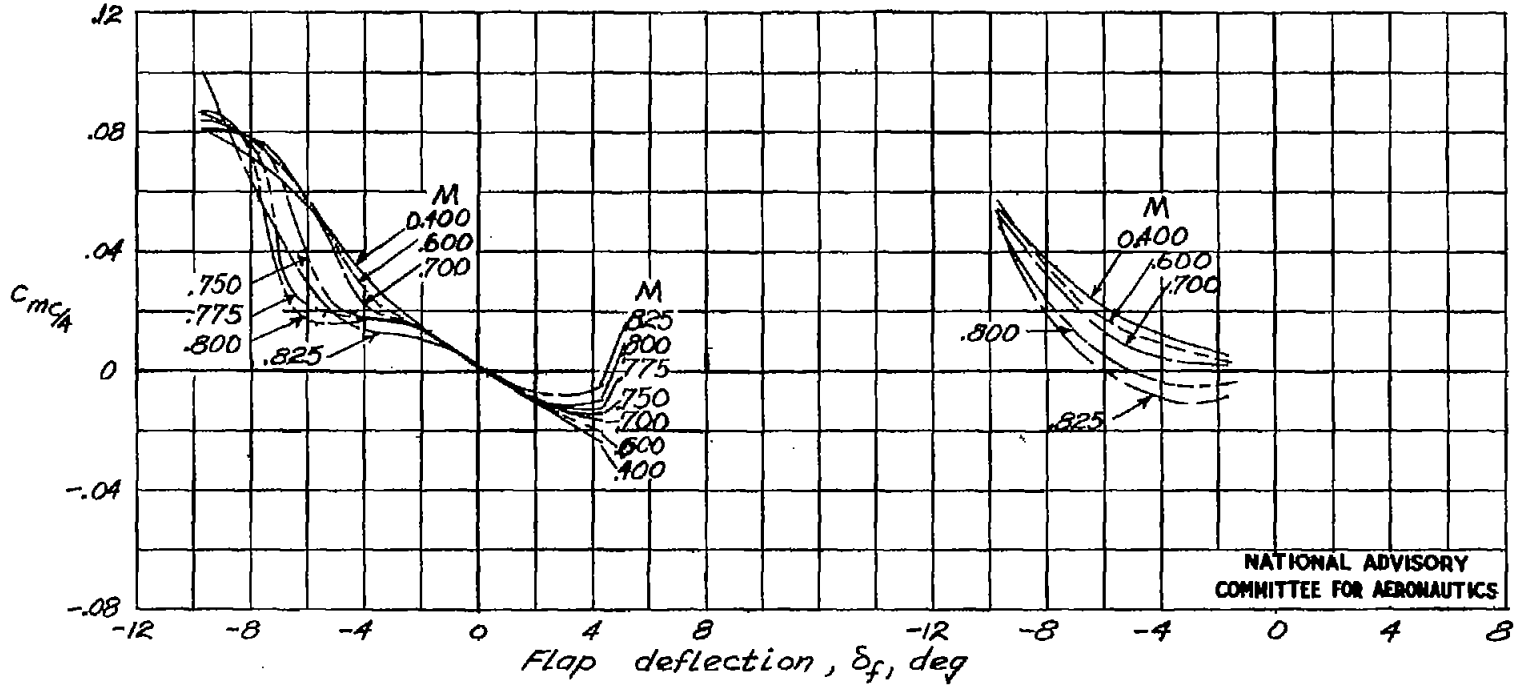

(a) $\alpha = 0^\circ$. (b) $\alpha = 0^\circ$. Leading edge roughened.

Figure 11.- Variation of section quarter-chord moment coefficient with flap deflection.

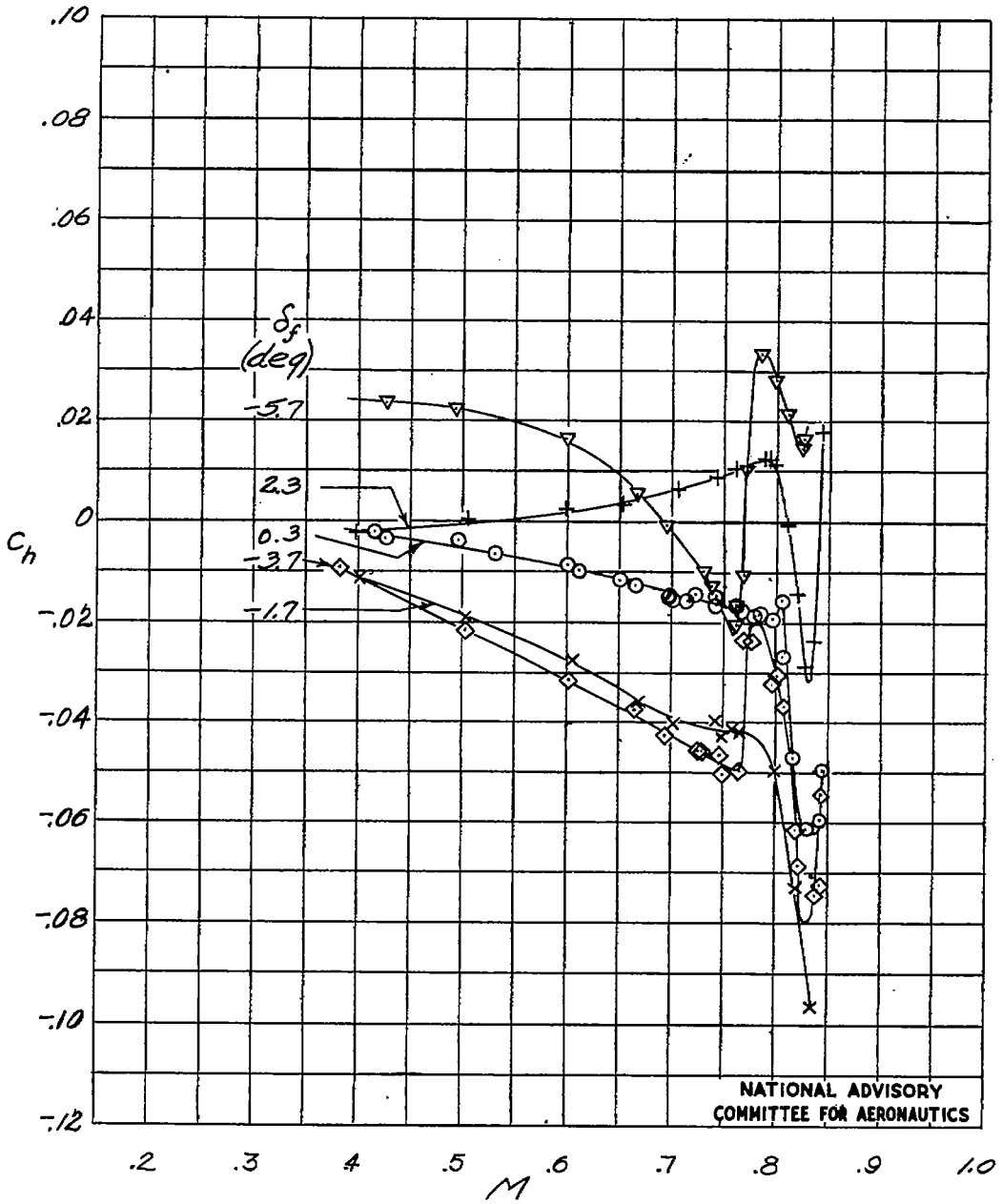

(a) $\alpha = -2^\circ$.

Figure 12.- Variation of flap section hinge-moment coefficient with Mach number.

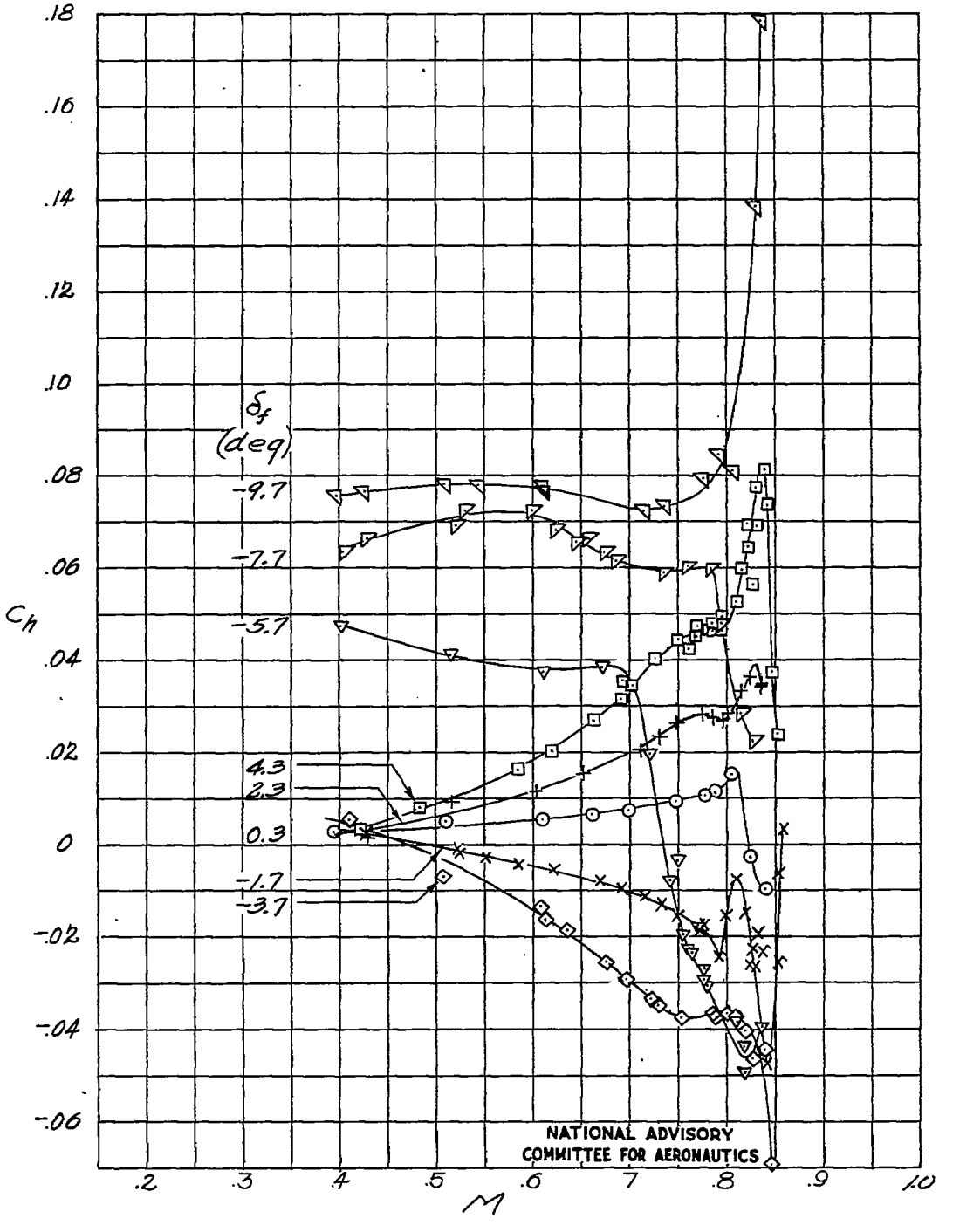

(b) $\alpha = 0^\circ$.

Figure 12.- Continued.

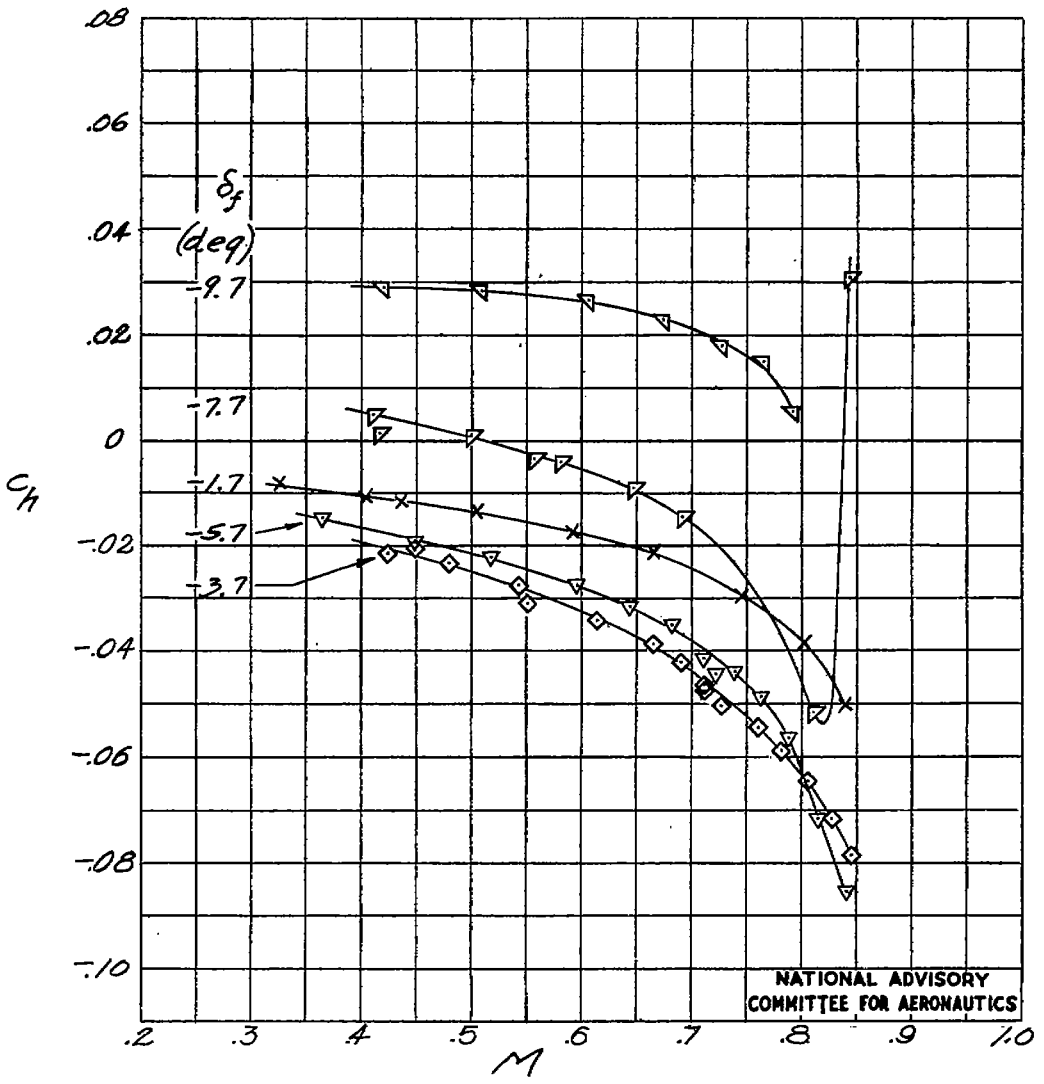

(c) $\alpha = 0^\circ$. Leading edge roughened.

Figure 12.- Continued.

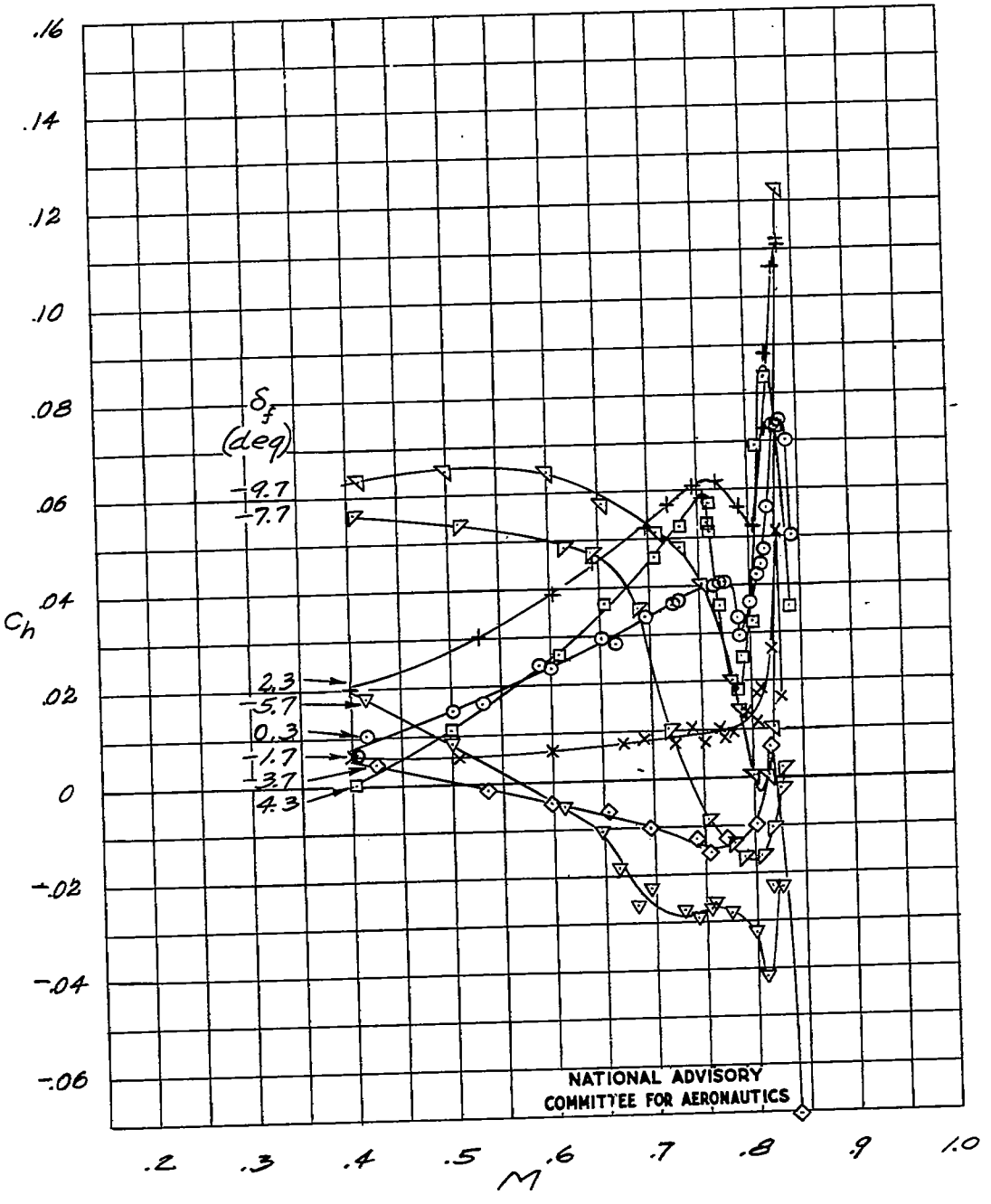

(d) $\alpha = 2^{\circ}$.

Figure 12.- Continued.

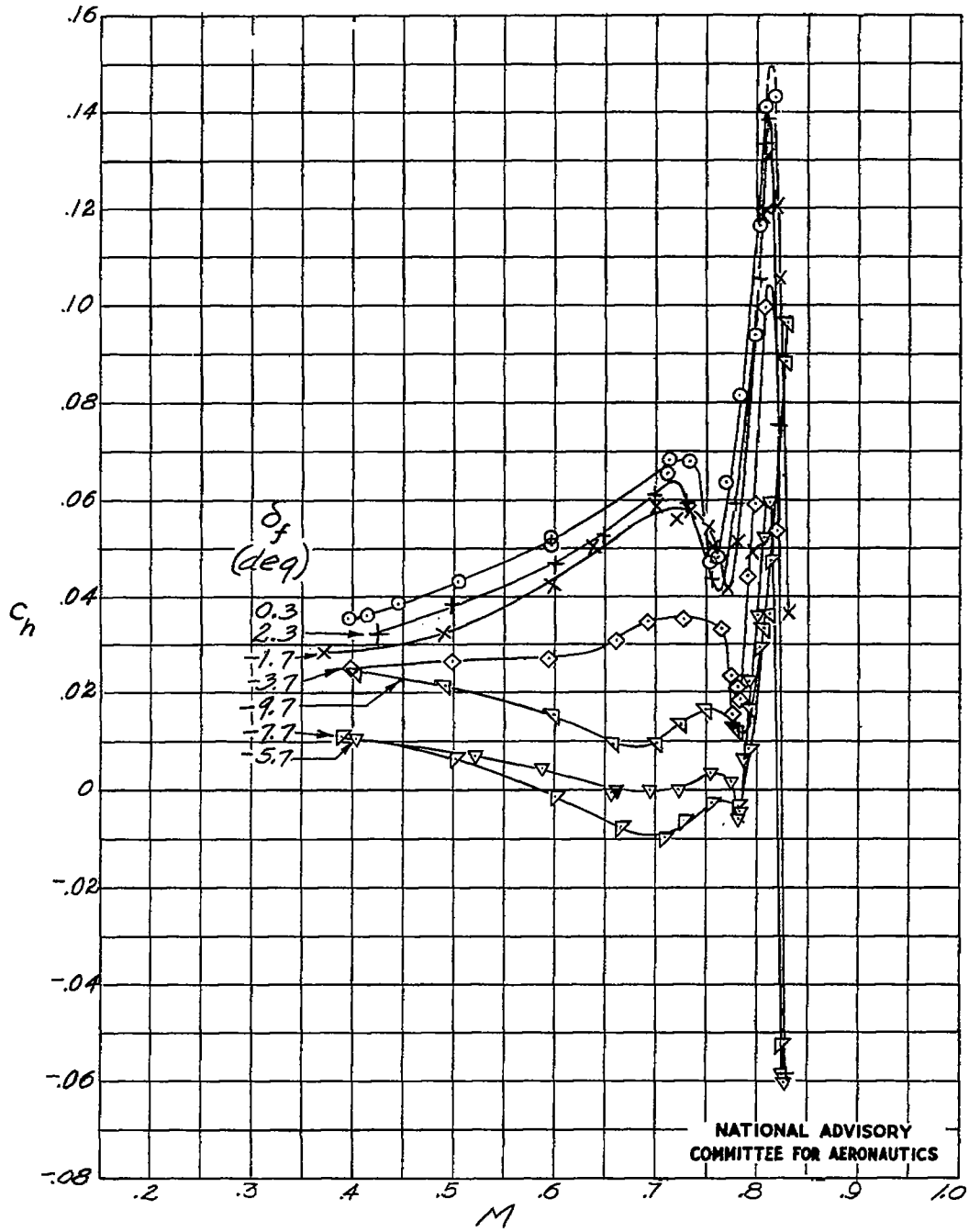

(e) $\alpha = 4^\circ$.

Figure 12.- Continued.

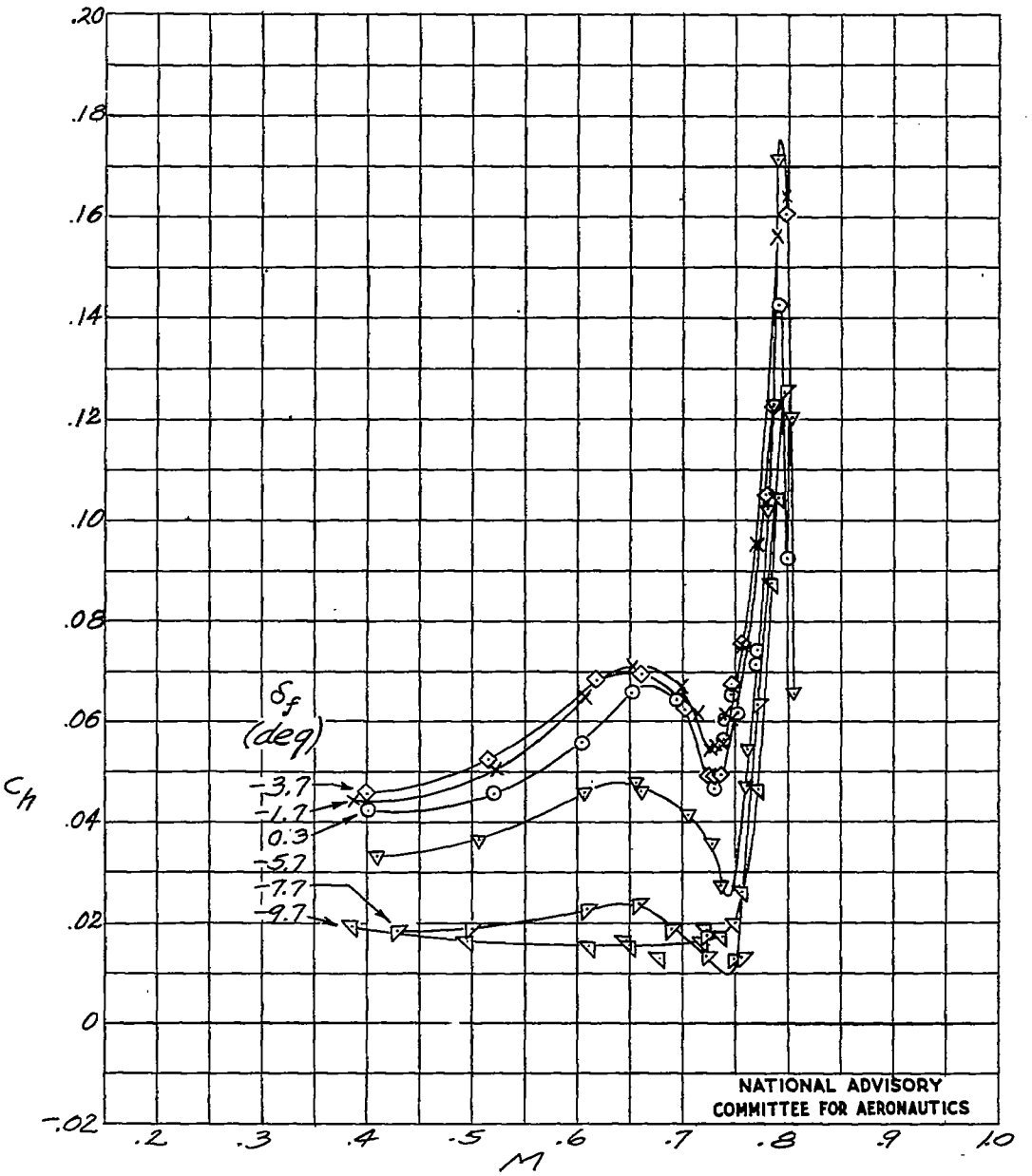

(f) $\alpha = 6^\circ$.

Figure 12.- Concluded.

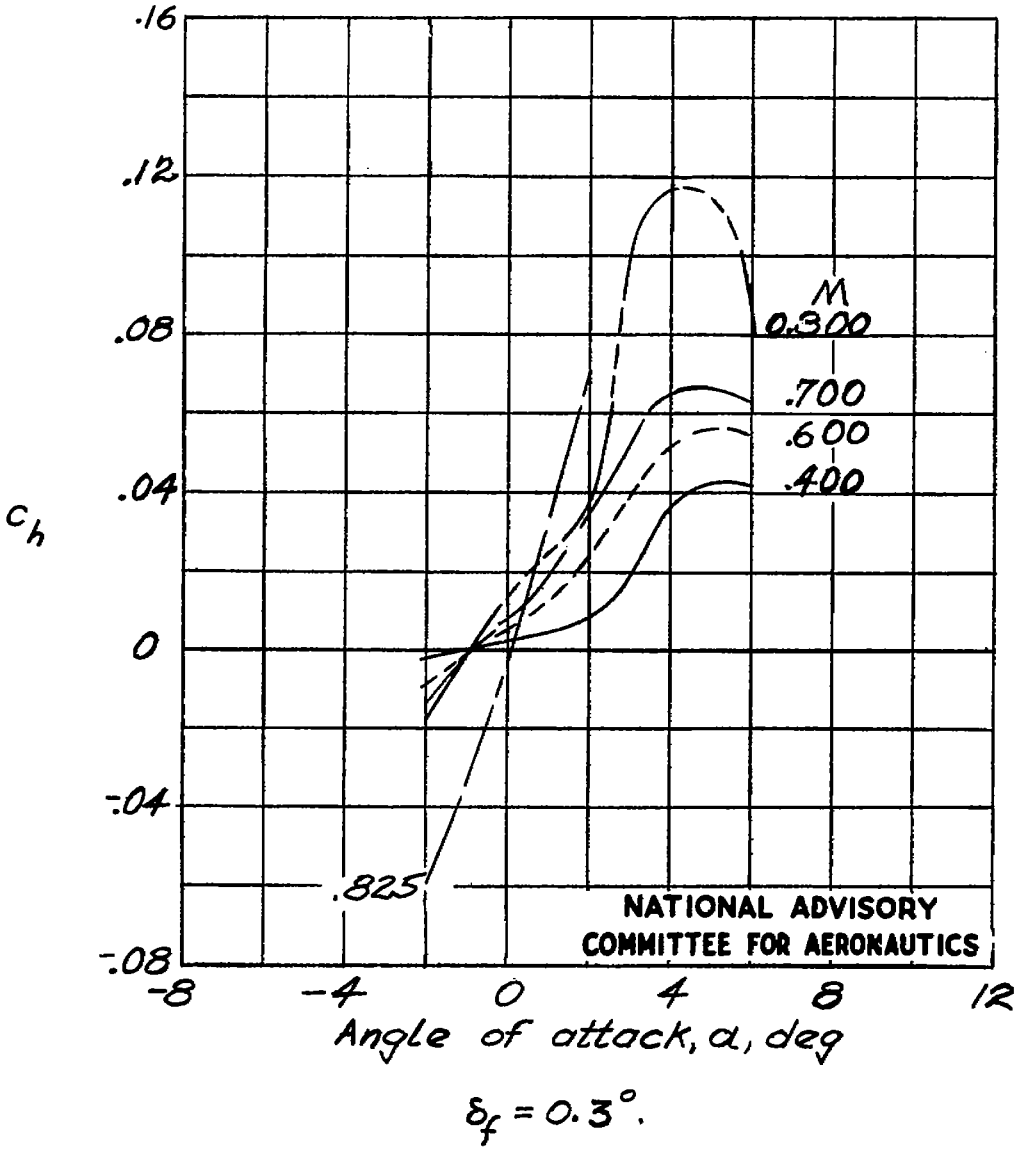

Figure 13.- Variation of flap section hinge-moment coefficient with angle of attack. $\delta_f = 0.3°$.

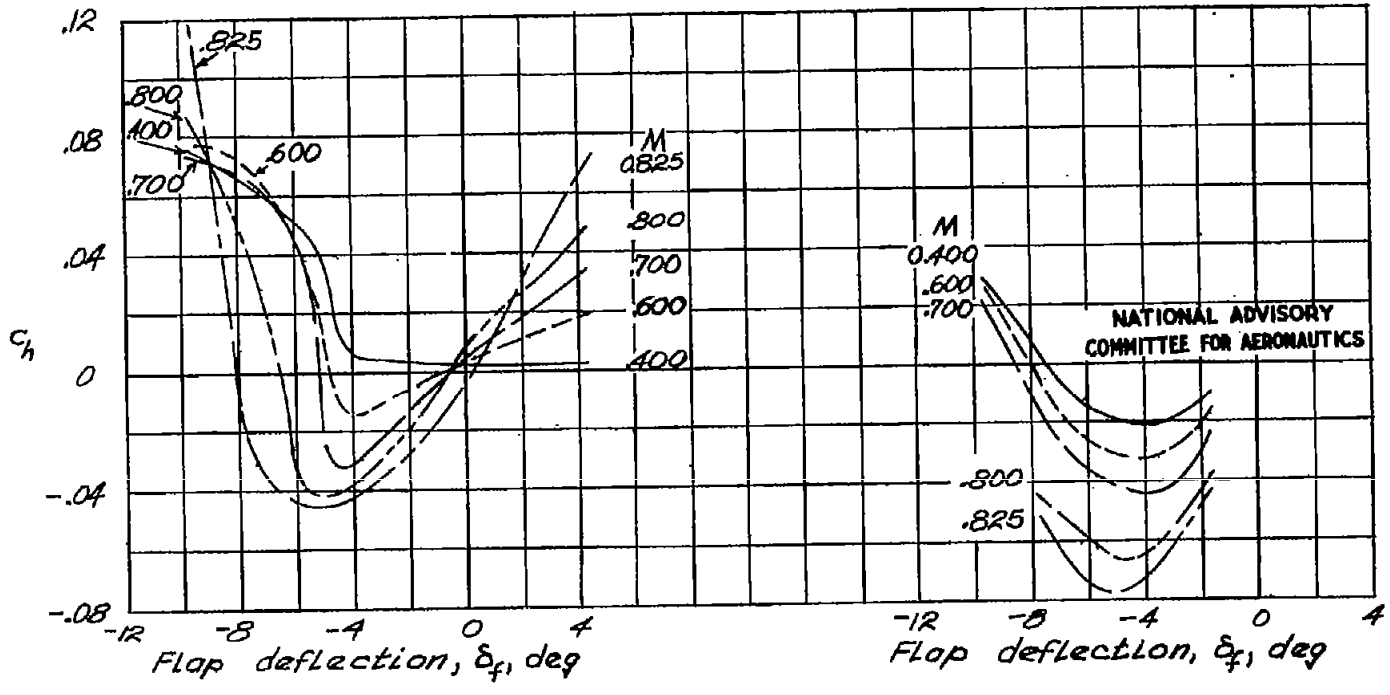

(a) $\alpha = 0^\circ$. (b) $\alpha = 0^\circ$. Leading edge roughened.

Figure 14.- Variation of flap section hinge-moment coefficient with flap deflection.

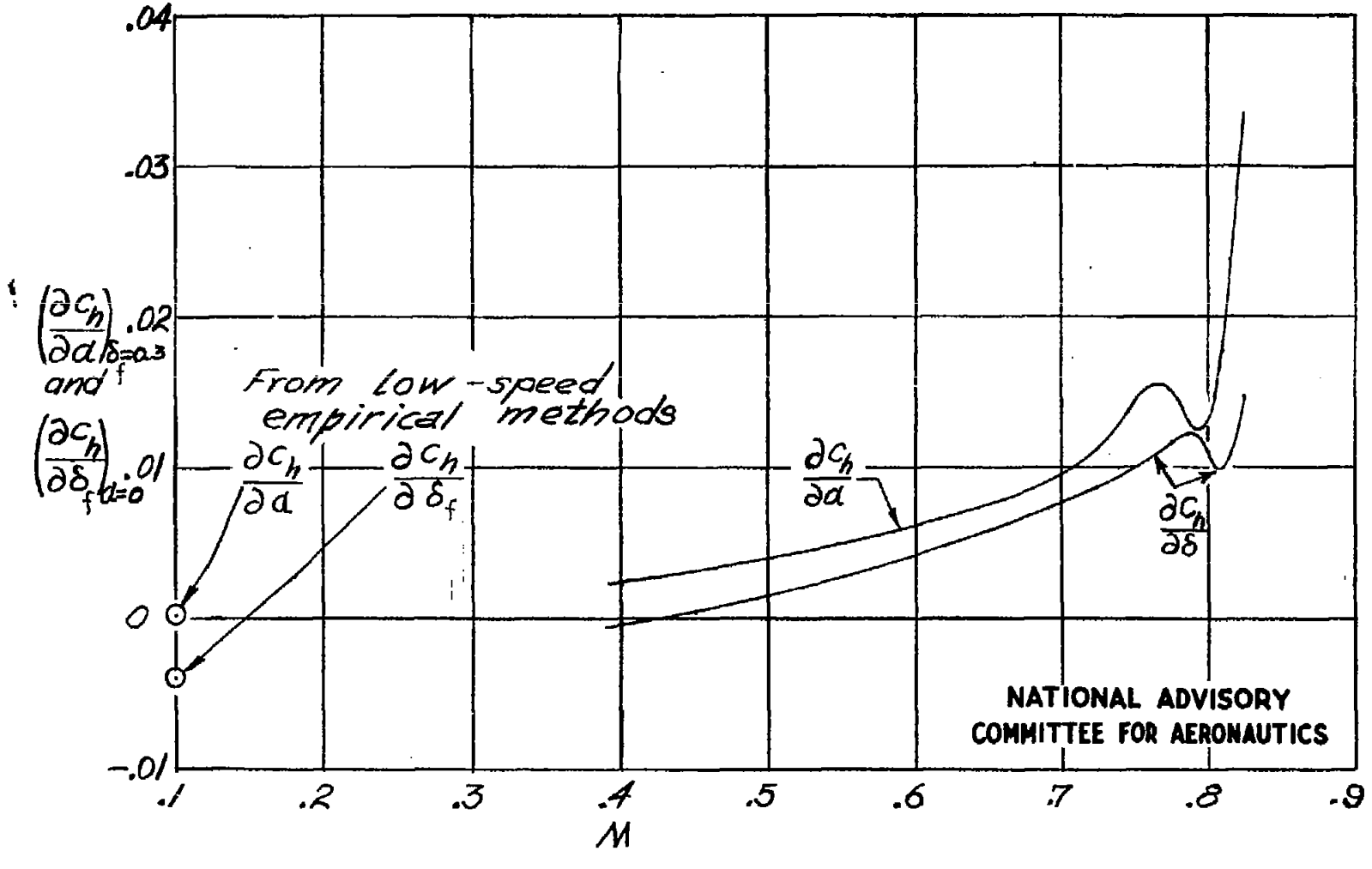

Figure 15.- Variation of hinge-moment slopes with Mach number.